



Facies analysis and basin architecture of the Neogene Subandean synorogenic wedge, southern Bolivia

Cornelius Eji Uba^{*}, Christoph Heubeck, Carola Hulka

Institut für Geologische Wissenschaften, Freie Universität Berlin, Malteserstrasse 74-100, 12249 Berlin, Germany

Received 20 January 2005; received in revised form 31 May 2005; accepted 30 June 2005

Abstract

Foreland sedimentation in the Subandean Zone of south-central Bolivia spans from the Upper Oligocene to present. It records sediment dispersal patterns in an initially distal and later proximal retroarc foreland basin, and thereby contains stratigraphic information on the tectonic evolution of the adjacent Andean fold-thrust belt. Within the Neogene orogenic wedge individual siliciclastic-dominated depositional systems formed ahead of an eastward-propagating deformation regime.

We defined, described, and interpreted eight architectural elements and 24 lithofacies from 15 outcrop locations representing the Neogene foreland basin in the Subandean Zone and the Chaco Plain. These are combined to interpret depositional settings. The up to 7.5 km-thick Neogene wedge is subdivided in five stratigraphic units on the basis of facies associations and overall architecture: (1) The basal, Oligocene–Miocene, up to 250 m-thick Petaca Formation consists dominantly of calcrete, reworked conglomeratic pedogenic clasts, and fluvial sandstone and mudstone. This unit is interpreted to represent extensive pedogenesis under an arid to semiarid climate with subordinate braided fluvial processes. (2) The overlying, Upper Miocene, up to 350 m thick Yecua Formation records numerous small-scale transgressive–regressive cycles of marginal marine, tidal, and shoreline facies of sandstone, ooid limestones, and varicoloured mudstone. (3) The Upper Miocene, up to 4500 m-thick Tariquia Formation principally consists of sandstone with interbedded sandstone–mudstone couplets representing frequent crevassing in anastomosing streams with an upsection-increasing degree of connectedness. (4) The up to 1500 m-thick Lower Pliocene Guandacay Formation represents braided streams and consists principally of granule to cobble conglomerate interbedded with sandstone and sandy mudstone. (5) The Upper Pliocene, up to 2000 m-thick Emborozu Formation consists predominantly of alluvial-fan-deposited cobble to boulder conglomerate interbedded with sandstone and sandy mudstone.

The coarsening- and thickening-upward pattern and eastward progradation, coupled with the variable proportions of overbank facies, channel size, and degree of channel abandonment, in the Tariquia, Guandacay, and Emborozu Formations reflect a distal through proximal fluvial megafan environment. This long-lived megafan grew by high sedimentation rates and a northeast-through-southeast radial paleoflow pattern on large, coarse-grained sediment lobes. The marked overall

^{*} Corresponding author. Present address: Institut für Geowissenschaften, Universität Potsdam, Postfach 601553, D-14415 Potsdam, Germany.
E-mail address: ejikeuba@zedat.fu-berlin.de (C.E. Uba).

upsection change in pattern and depositional styles indicate fluctuations in accommodation space and sediment supply, regulated by basin subsidence, and are attributable to Andean tectonics and climatic controls.

© 2005 Elsevier B.V. All rights reserved.

Keywords: Neogene; Fluvial and marine sequence; Architectural analysis; Foreland; Basin history

1. Introduction

Neogene strata of the Subandean Zone (SZ) and the easterly adjacent Chaco Plain (CP) represent dominantly alluvial–fluvial deposits that accumulated within a foreland basin setting on the eastern side of the Andes in response to eastward propagation of the Andean fold-and-thrust belt (Fig. 1). This retroarc foreland basin formed as a result of Mesozoic–Recent subduction of the Nazca and Pacific plates, accompanied by Oligocene–Recent uplift of the Andean Cordillera (Isacks, 1988; Kley et al., 1997; Sempere et al., 1990; Kley et al., 1999). The Upper Oligocene–Recent sedimentary strata representing this rapid eastward Andean growth are particularly

well exposed in the Subandean foothills. Although the SZ and the adjacent CP represent one of the classical foreland systems in South America, no detailed sedimentological study has yet been conducted despite the good outcrop quality and the long history of petroleum exploration and production expressed in numerous publications on the petroleum systems and hydrocarbon potential of the SZ (Baby et al., 1995; Dunn et al., 1995; Moretti et al., 1996). In contrast, a wealth of information exists on the structural styles, geometry, and tectonic history of the Subandean belt (Sempere et al., 1990; Baby et al., 1992, 1994; Welsink et al., 1995; Kley, 1996; Colletta et al., 1999; Kley, 1999; Echavarría et al., 2003), including aspects of its subsidence, uplift, and

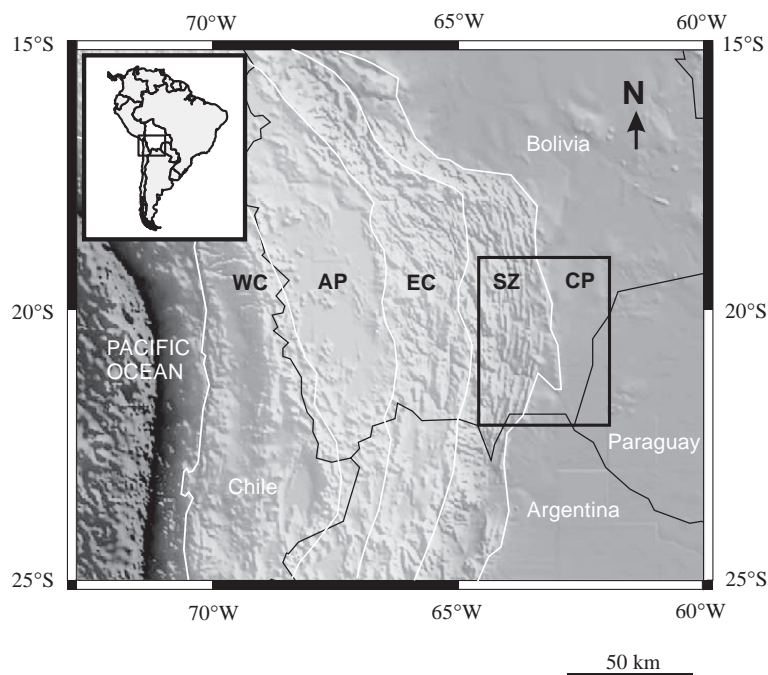


Fig. 1. Topographic map of the Central Andes showing major morphotectonic divisions and location of the study area. WC Western Cordillera, AP Altiplano, EC Eastern Cordillera, SZ Subandean Zone, CP Chaco Plain.

thermal history (Isacks, 1988; Gubbels et al., 1993; Coudert et al., 1995; Beck et al., 1996; Husson and Moretti, 2002; Ege, 2004).

This study attempts to provide the first comprehensive sedimentological analysis of the Neogene

units in the SZ and the CP. The objectives of this study are (1) to provide a detailed sedimentary facies analysis and account for the depositional architecture of the Neogene Subandean synorogenic strata, (2) document the responses to tectonic episodes in sedi-

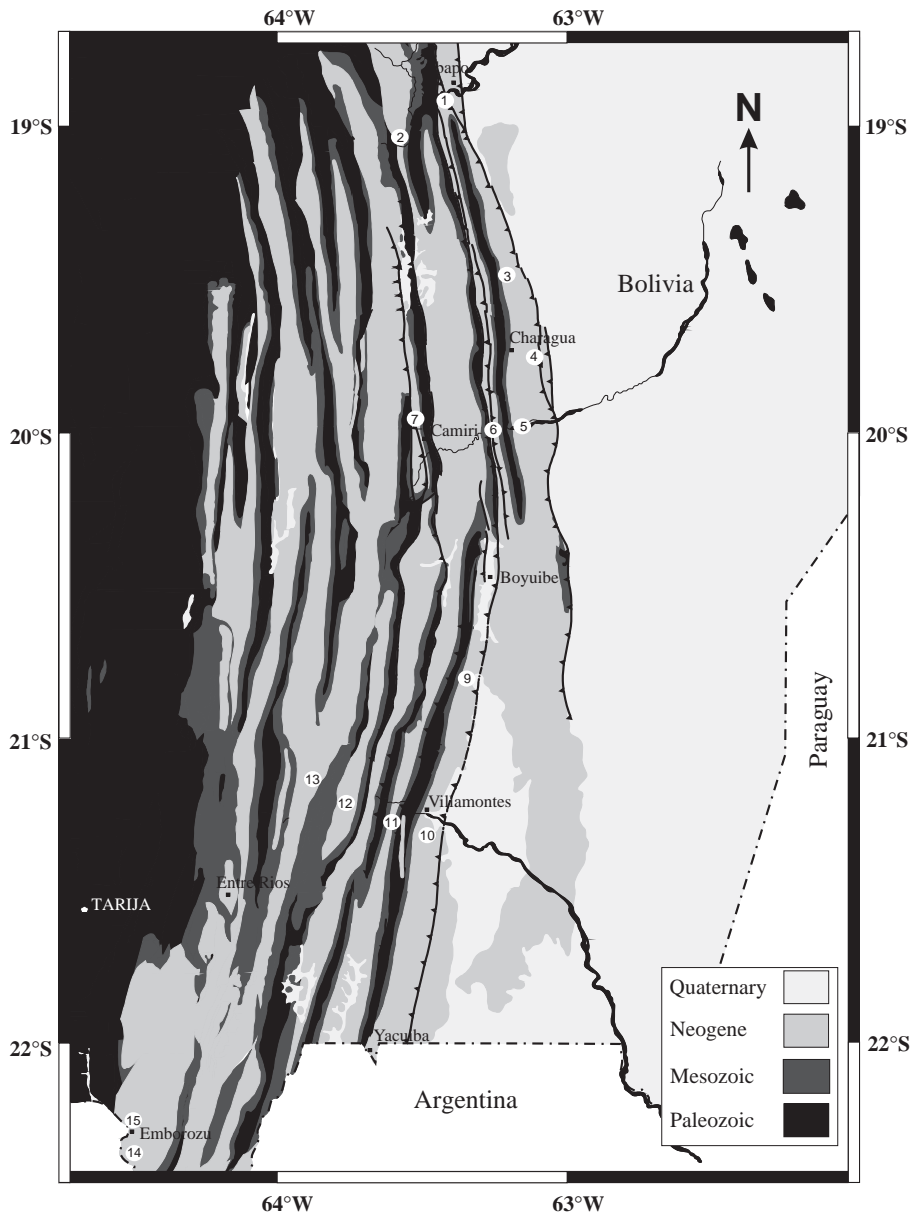


Fig. 2. Geological and structural map of the study area (modified after Suarez Soruco, 1999) showing the localities of measured sections mentioned in the text: 1. Abapo, 2. Tatarenda, 3. Saipuru, 4. Piriti, 5. San Antonio, 6. Oquitas, 7. Choreti, 8. Iguamirante, 9. Machareti, 10. Angosto del Pilcomayo (Villamontes), 11. Puesto Salvacion, 12. Zapaterimbia, 13. Rancho Nuevo, 14. Nogalitos, and 15. Emborozu.

mentary facies patterns, and (3) to characterize and identify sediment sources and supply. These objectives will provide insights into Andean uplift history (and the related eastward migration of the deformation front) and the interaction between tectonics and sedimentation pattern. In addition, a paleoenvironmental analysis is critical in understanding the paleoclimate.

2. Geological setting

The Chaco basin stretches east–west from the Main Frontal Thrust (MFT [Sempere et al., 1990](#)) to its onlap on the Brazilian Shield. The western third of this basin is deformed as a fold-and-thrust-belt and therefore well exposed. This section is known as the Subandean Zone (SZ). Beyond its morphotectonic eastern limit near 63°W ([Fig. 2](#)), the Subandean Zone continues into the presently undeformed and topographically flat foreland, covered by Quaternary deposits of the Chaco Plain (CP). [Coudert et al. \(1995\)](#) estimated the E–W width of the undeformed foreland basin at 100 to 120 km. Our study area in southern Bolivia

([Figs. 1 and 2](#)) is limited to the east by the eastern front of the Subandean fold-and-thrust belt ([Oller, 1986; Sheffels, 1988; Baby et al., 1992; Hérail et al., 1996](#)) and to the west by the Main Frontal Thrust, where tilted Neogene strata are commonly well exposed along the flanks of its major syn- and anticlines ([Fig. 2](#)).

The evolution of the Chaco basin is closely related to the evolution of the Altiplano of the central Andes. Sedimentation in the Neogene Chaco foreland basin commenced in the Upper Oligocene ([Marshall and Sempere, 1991; Gubbels et al., 1993; Jordan et al., 1997; Kley et al., 1997](#)), when the deformation front began its eastward propagation from the Eastern Cordillera. Since the Upper Miocene (~10 Ma), the basin was affected by major shortening ([Gubbels et al., 1993](#)). The Recent deformation front is marked by a complex blind thrust beneath the foothills several tens of kilometers east of the present topographic front of the Subandean belt ([Baby et al., 1992; Roeder and Chamberlain, 1995](#)). The Subandean Belt is composed of basement-involved faults blocks that develop laterally into thin-skinned thrust sheets and

Age (Ma)	Epoch	Formation		Thickness (m)
		Subandean	Chaco	
~3.3	Late Pliocene–Pleistocene	Emborozu Fm		500 - 2000
	Late Late Miocene–Late Pliocene	Guandacay Fm		500 - 1500
~6	Late Late Miocene	Tariquia Fm		1200 - 4500
~7	Late Miocene	Yecua Fm		0 - 350
~14	Oligocene–Middle Miocene	Petaca Fm		10 - 250
~27	Cretaceous			

Fig. 3. Tertiary chronostratigraphy of the Subandean Zone and Chaco basin fill. The formation ages are based on [Marshall and Sempere \(1991\)](#), [Moretti et al. \(1996\)](#), and [Hulka et al. \(in press\)](#).

show elongated N–NE trending ramp anticlines (Belotti et al., 1995; Kley et al., 1996, 1999) and passive roof duplexes (Baby et al., 1992), separated by thrust faults and synclines. Baby et al. (1997) suggest 140 km (20°S) to 86 km (22°S) of shortening (~36%) within the SZ.

Deposition of the Subandean synorogenic wedge, which unconformably overlies largely eolian Mesozoic strata, began in the Upper Oligocene at ~27 Ma (Gubbels et al., 1993; Sempere et al., 1990). It reaches a maximum thickness of ~7.5 km in the southern part of the study area and includes dominantly nonmarine red beds (with the exception of the brackish-shallow marine Yecua Formation), which have conventionally been classified into five stratigraphic units, largely on lithostratigraphic grounds (Fig. 3). The up to 250 m-thick, Deseadean-to Chasicuan-age (Sempere et al., 1990; Marshall and Sempere, 1991; Marshall et al., 1993) Petaca Formation consists of calcrete, sandstone, and mudstone. The up-to-350 m-thick Yecua Formation represents a marine incursion (Padula and Reyes, 1958; Marshall et al., 1993). Marshall et al. (1993) constrained the Yecua age using biostratigraphy at 10–8 Ma, while Hulka et al. (in press) estimated its depositional age at 14–7 Ma. Overlying this formation is the Upper Miocene (Moretti et al., 1996), ~4500 m-thick, sandstone- and mudstone-dominated Tariquia Formation. The conglomerate-dominated Upper Miocene to Quaternary (Moretti et al., 1996) up to 1500 m-thick Guandacay and up to 2000 m-thick Emborozu formations cap the Neogene stratigraphic column.

3. Methods

This study is based on the integration of lithologic, sedimentologic and biostratigraphic data collected during three field seasons in the SZ and CP in southern Bolivia. We profiled and sampled 15 stratigraphic sections (see Fig. 2 for names and locations) along major rivers (Rio Pilcomayo, Rio Parapeti, and Rio Bermejo), small streams (e.g. Quebrada Machareti), and road cuts (Tarija–Bermejo). Analysis of photo mosaics and field tracing of individual strata to document lateral and vertical stacking patterns and facies distribution supplement-

ted field interpretations. In addition, more than 250 paleocurrent indicators were measured to constrain dispersal patterns.

4. Lithofacies and architectural elements

Lithofacies and architectural elements were defined based on sedimentary structures, lithology, pedogenic features, and fossils. We used modified lithofacies and architectural classifications from Miall (1985, 1996) and Einsele (2000) for facies analysis and established a total of 24 lithofacies types, 8 architectural elements, and 15 facies associations (P1-4, Y1-3, T1-3, G1-3, and E1-2 respectively) (Tables 1, 2 and 3). The recognition of architectural elements, their characteristics, and relationship permit us to understand depositional settings and the probable processes that may have influenced the development of the marine and non-marine systems. The architectural elements are defined on the basis of sets of large-scale stratal characteristics or by groups of genetically related strata sets, grain sizes, constituent lithofacies, and vertical and lateral relationships of each element (Miall, 1985, 1996). The various architectural elements identified in the study area are described and interpreted (Table 2).

4.1. Petaca Fm

The Petaca Formation (Birkett, 1922) marks the onset of Neogene foreland sedimentation in the Subandean Zone and Chaco Plain (Sempere et al., 1990). A transitional contact, or in places a very low-angle basal unconformity, defines the contact of the Neogene successions with the underlying Cretaceous Tacuru Group, which is dominated by large-scale trough-cross-bedded eolian sandstone. This unconformity is rarely recognizable in the field but is discernible on seismic sections (Moretti et al., 1996; Uba et al., submitted for publication). In the study area, the up to 250 m-thick Petaca Formation consists of four facies associations: (1) basal paleosol (P1), (2) reworked pedogenic conglomerate (P2), (3) sandstone (P3), and (4) mudstone (P4; Fig. 4, Table 3), which are best represented in the Iguamirante section.

Table 1
Description and interpretation of sedimentary facies (after Miall, 1985, 1996; Einsele, 2000)

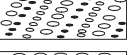
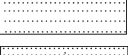
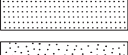
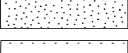
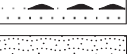
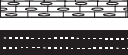
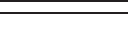
Facies code	Characteristic	Interpretation
Gmd	 Disorganised, matrix-supported polymictic conglomerates. Boulder and pebbles, subangular to rounded. 1 to 10 m thick	Mass flows deposited from hyperconcentrated or turbulent flow
Gcd	 Disorganised, clast-supported polymictic conglomerates. Boulders and pebbles subangular to rounded. 1 to 8 m thick.	Rapid deposition by stream-floods with concentrated clasts
Gco	 Organised, clast-supported polymictic conglomerates. Cobble and pebbles, inverse to normal grading, weak imbrication.	Traction bedload, transported by persistent fluvial stream
Gt	 Clast-supported trough cross-stratified conglomerates. Cobble and granules, normal grading with imbrication	Transverse bar, channel fill
Gp	 Clast-supported planar cross-stratified conglomerates. Cobble and granules, subrounded to rounded	Linguoid bar, transverse bar
Gh	 Clast-supported horizontally bedded conglomerates. Cobble and granules, normal to inverse grading with imbrication	Longitudinal bedforms, lag deposit, sieve deposit
St	 Trough cross-stratified sandstone. Very fine to coarse-grain size, occasionally pebbly	Dune migration, lower flow regime
Sp	 Planar cross-stratified sandstone. Very fine to coarse-grain size, occasionally pebbly, moderate to well sorting	2D dunes, lower flow regime
Sh	 Horizontally stratified sandstone. Very fine to coarse-grain size, occasionally with pebbles, moderate to well sorting	Planar bed flow, upper flow regime
Sl	 Laminated-stratified sandstone. Very fine to medium-grain size, occasionally with pebbles, well sorting	Antidunes, upper flow regime
Sm	 Massive sandstone. Very fine to coarse-grain size, pebbly, moderate to well sorting	Rapid deposition, sediment gravity flow
Ss	 Scour surface. Very fine to coarse-grained sandstone and conglomerates, filled with interformational mudclast	Scour fills
Sr	 Ripple cross-stratified sandstone. Very fine to medium-grain size, occasionally pebbly and climbing ripple, moderate sorting	2D or 3D ripples, upper flow regime
Smf	 Flaser bedded sandstone. Fine to medium-grain size, occasionally pebbly and climbing ripples, moderate sorting	Suspension settling to low flow regime
Smw	 Wavy bedded sandstone. Fine to medium-grain size, occasionally pebbly and ripples, moderate sorting	Suspension settling to low flow regime
Sml	 Lenticular bedded sandstone. Fine to medium-grain size, occasionally pebbly and ripples, moderate sorting	Suspension settling to low flow regime
Smh	 Herringbone cross-stratified sandstone. Fine to medium-grain size, occasionally pebbly, moderate sorting	Suspension settling to low flow regime
Shc	 Convolute bedded sandstone. Fine to medium-grain size, moderate sorting	Deformation by differential loading
Shs	 Shell-dominated calcareous sandstone. Parallel orientation, fine to medium-grain size	Suspension deposits
Fl	 Fine laminated. Mudstone to siltstone. Occasionally calcareous and contain mica flakes	Suspension deposits, overbank or abandoned channel
Fm	 Massive or platy. Mudstone to siltstone. Occasionally calcareous	Suspension deposits, overbank or abandoned channel
Fb	 Bioturbated. Mudstone to siltstone. Abundant burrows, destruction of fabric	Overbank or abandoned channel, incipient soil
P	 Pedogenic calcretes. Strongly developed, massive, occasionally crude lamination	Mature paleosol
C	 Coal, carbonaceous mud, plant remains	Vegetated swamp deposit

Table 2

Description and interpretation of fluvial architectural elements in the Chaco foreland basin

Architectural element	Grain size	Description	Interpretation
Channel-fill complex (CH)	Pebble to cobble conglomerate, fine-to coarse-grained sandstone with mudclasts	Lenticular, multi- and single-storeys, sharp concave-up erosive base, lateral extent up to 150 m. Gco, Gt, Gh, Gp, St, Sh, Sp, Sm, Ss, and Sr	Growth of gravelly and sandy channel fills
Gravel bars (GB)	Clast-supported granules to cobble conglomerate interbedded with sandstone	Sheet-like and lens, more than 100 m lateral extent. Gco, Gt, Gp	Gravel sheets and lens, relative low-relief longitudinal bars
Downstream-accretion (DA)	Granule to pebble conglomerate, fine-to coarse-grained sandstone	Wedge-like, tens of meters in lateral extent. Gh, Sh, St, Ss, and Sp	Downstream accretion of gravel and sand bars
Sediment gravity flows (SG)	Matrix- to clast-supported pebble to boulder conglomerate	Lobe- or sheet-like, interbedded with GB and SB. Gmd and Gcd	Lobe, sheet gravel gravity flow
Sandy bedform (SB)	Fine- to coarse-grained sandstone	Vertical stack, wedge or sheet-like, with erosional surfaces, lateral extent up to 50 m. St, Sp, Sh, Sl, Sr, Ss, and Sm	Channel fills, dunes, and crevasse splay
Laminated sand sheet (LS)	Very fine- to medium-grained sandstone, with intraformational mudclasts	Sheet and minor blanket, erosive base, lateral extent of more than 150 m. Sh, Sl, Sr, St, and Ss	Flash flood deposits, crevasse splay, upper flow-regime
Crevasse channel (CR)	Fine- to coarse-grained sandstone with intraformational mudclasts	Ribbon, up to few 100s of meters wide, up to 3 m thick. St, Sr, and Ss	Sandy crevasse channel fill
Overbank fines (OF)	Mudstone and very-to fine-grained sandstone	Sheet-like, lateral extent for more than 200 m. Sr, Sl, Fl, Fm, Fb, Fd and C	Overbank and floodplain

Modified from Miall (1985, 1996).

4.1.1. P1. Basal paleosol

4.1.1.1. Description. The lower part of the Petaca Formation is dominated by up to 22-m-thick calcrete, reaching a maximum thickness in Iguamirante section (Fig. 4A). The calcrete displays abundant, in-situ, white to greenish gray (rarely light purple) calcareous nodules in a brown to light-red sandstone matrix. The nodules occur isolated, clustered, or coalesced. Their forms vary from spherical to irregular, blocky, and massive, or are pseudo-prismatic due to fracturing and brecciation (Fig. 4D). Nodule-bearing paleosols are dominantly interbedded with intraformational, nearly monomict nodule conglomerate, which may also include a few chert and quartzite pebbles, and occasionally with well-cemented, decimeter-thick, cross-stratified, light brown to white sandstone. Fractures and voids are generally filled either with host sediment or calcite.

In the southern part of the study area (Nogalitos section, Fig. 2), the Petaca calcrete consists of varicolored, olive to turquoise, spherical or laminated nodules aligned parallel to bedding planes. They are characterized by polygonal desiccation cracks filled with coarse-grained sandstone and appear altered by

hydrothermal fluids. The Petaca basal paleosol facies association consists of P and Sh lithofacies (Table 1).

4.1.1.2. Interpretation. The presence of carbonate nodules with soil profiles and sharp boundaries may reflect a pedogenic origin, having formed by downward leaching or precipitation of calcium carbonate (e.g. Khadkikar et al., 2000). The association of carbonate nodules with host rock sandstone, their prismatic appearance, and high degree of pedogenesis suggest a fossil B horizon (Wright and Tucker, 1991; Wright, 1994) of a vertic calcisol of stage III/IV (Gile et al., 1966; Machette, 1985; Mack et al., 1993) which probably formed due to reduced sediment availability under a climate with long dry and relatively short wet seasons (e.g. Cecil, 1990). This resulted in upward-directed groundwater flow and mineral precipitation in the B horizon. Floating and embayed detrital grains indicate near-surface pedogenic activity. These are well-documented in modern and ancient soils of fluvial deposits (e.g. Retallack, 1990; Pimentel et al., 1996; Khadkikar et al., 2000). The well-cemented sandstone interbeds are interpreted as starved eolian sand dunes. Over-

Table 3
Facies associations and their occurrences in the Neogene Subandean wedge

Facies association	Lithofacies	Architectural elements	Thickness (m)	Interpretation and dep. environment	Occurrence
P1: Basal paleosol	P, Sh	LS, CH	2–20	Pedogenesis	Petaca
P2: Reworked pedogenic unit	Gcd, Gh	SG, GB, SB	1–5	Gravelly fluvial (braided)	Petaca
P3: Sandstone	Sm, St, Sh, Sp, Ss	CH, SB, DA	5–45	Sandy fluvial (braided)	Petaca
P4: Mudstone	Fl, Fm	OF	0.5–2	Overbank and suspended fluvial (braided)	Petaca
Y1: Laminated interbedded sand-stone and mudstone	SMf, SML, SMw, Smh, Sr	–	>50	Tidal	Yecua
Y2: Pebbly calcareous sandstone	Sp, Sr	–	>5	Shoreline	Yecua
Y3: Fossiliferous varicolored mud-stone	ShS, Mp, Sl	–	>10	Shallow marine	Yecua
T1: Thick channelized sandstone	Sm, St, Sp, Sh, Sl, Sr, Ss	CH, SB, LS,	5–20	Fluvial major channel (anastomosing distal fluvial megafan)	Tariquia
T2: Thin sandstone	Sm, St, Sh, Sr, Ss	SB	0.5–5	Crevasse channel (anastomosing distal fluvial megafan)	Tariquia
T3: Interbedded mudstone and sandstone	Sl, Sr, Ss, Fl, Fm, Fb, Fd, C	CH, SB, LS, OF	2–60	Mud-dominated overbank (anastomosing distal fluvial megafan)	Tariquia
G1: Granule-cobble conglomerate	Gco, Gcd, Gh, Gt, Gp	GB, CH, LA	1–10	Gravelly braided channel (mid fluvial megafan)	Guandacay
G2: Coarse-grained sandstone	Sh, Sp, St, Ss	CH, SB, LA	0.5–10	Sandy braided channel (mid fluvial megafan)	Guandacay
G3: Interbedded sandstone and mudstone	Sr, Sm, Sl, Fl, Fm, Fb, C	LS, OF	1–40	Sand-dominated overbank (mid fluvial megafan)	Guandacay and Emborozu
E1: Cobble-boulder conglomerate	Gmd, Gcd, Gco	GB, CH, LA	3–60	Large alluvial fan (proximal fluvial megafan)	Emborozu
E2: Sheet-like sandstone	Gco, Sp, Sh, St, Ss	CH, SB, LA	2–6	Large alluvial fan (proximal fluvial megafan)	Emborozu

all, the Petaca paleosols indicate sharply reduced or absent sedimentation for long time periods on surfaces in an arid to semi-arid paleoclimate, in which evaporation exceeded precipitation.

4.1.2. P2. Reworked pedogenic conglomerate

4.1.2.1. Description. The reworked pedogenic conglomerate facies association is characterized by horizontal to disorganised clast-supported conglomerate (Gcd and Gh; Fig. 4C). The poorly sorted and densely packed clasts consist principally of poorly rounded intraformational reworked calccrete nodules, with subordinate red subangular to subrounded chert and other extraformational granules and clasts up to 20 cm in diameter. This facies association shows variable bed thickness from 1 m (Machareti section, Fig. 2) to 2.5 m (Rancho Nuevo section, Fig. 2) due

to its sharp, moderately erosive bases. SG, SB, and GB are the principal architectural elements in this facies association (Table 2). The horizontal sheet-bedded gravel (Gh) dominates the internal fabric of the SB elements.

4.1.2.2. Interpretation. This facies association shows characteristics of stream flow deposits. Although the fabric of the conglomerate is reminiscent of debris flows, we interpret it as a product of rapidly decelerating, high-magnitude, gravel-dominated stream flow under flashy discharge. This interpretation is supported by the thick sheet-like structures, erosive boundaries, gravel clustering, poor sorting, absence of stratification, and rare to minor basal inverse grading (e.g. Nemeč and Steel, 1984). The nodules were apparently washed out of their soil horizons and transported only over short distances, as there is no clear evidence of

winnowing and sorting. Transport did apparently not form long-lived bedforms.

4.1.3. P3. Sandstone

4.1.3.1. Description. The 5 to 45 m-thick, calcareous, gray to reddish sandstone facies association overlies sharply but concordantly facies association P2 (Fig. 4B). This association is characterized by 1–15 m thick, medium- to very-coarse-grained sandstone with tabular beds, occasionally including medium-scale trough cross-beds (St), planar (Sp), massive (Sm), and crude horizontal (Sh) stratification, as well as intraformational mudclasts (Ss). They show a fining-upward trend and are moderately to well sorted, containing dispersed but horizontally oriented granules of reworked paleosol clasts and extraformational rock fragments. Occasional pebble trains loosely define horizontal stratification (Fig. 4C). The beds are lenticular in cross section and form channelized sand bodies in the upper part but stacked, laterally continuous sand sheets in the lower part of the sections. The architectural elements are shown in Table 2 and include channels (CH), laminated sheets (LS), and sand bedforms (SB). The sand bodies grade upward into mudstone.

4.1.3.2. Interpretation. We attribute this facies association to deposition from stream floods and/or waning flows because the constituent architectural elements (SB and LS) are indicative of variable high-energy flows and channel morphology. The laterally extensive lenticular sand bodies are interpreted as channel (CH) fills and indicate deposition in shallow scours during peak flood flow before waning flood conditions (Miall, 1996). The identified lithofacies (Sp, St, Sh) and lack of inclined, internally erosive surfaces suggest that sand bodies could be the vertically stacked product of confined, high-energy stream floods and record deposition associated with subaqueous dunes and upper-stage plane beds (Miall, 1996). The presence of pebble trains indicates that bedload transport of clasts occurred simultaneously with saltation and “wash-load” suspension fallout of sand grains. Several layers of interbedded gravel suggest fluctuations in flow strength during a single flow event. The fining-upward trend and change in

bedforms represent decreases in flow velocity or depth as frequency and intensity of floodwater events waned. The Se lithofacies represents bank erosion and high-energy stream flow (Miall, 1996; Bridge, 2003).

4.1.4. P4. Mudstone

4.1.4.1. Description. These fine-grained mud bodies consist of massive (Fm) and laminated (Fl) mud to sand (Table 1) and are characterized by the OF architectural elements. Individual mudstone and sandstone are laterally persistent, red to purple and range from 0.5 cm to 2 m in thickness. Bioturbation, subordinate small calcareous nodules, and minor desiccation cracks are occasionally present. The mudstone overlies the sandstone facies association, completing a fining-upward sequence.

4.1.4.2. Interpretation. This facies assemblage represents a mud-dominated floodplain or repeated mud drapes from a low-energy fluvial system. The laminated (Fl) geometry, proximity to channel sand bodies, and thin bed thickness is indicative of deposition in distal floodplains. The few-centimeter-thick Fm lithofacies therefore probably represents deposition from low-energy flows or from standing pools of water after channel abandonment (Miall, 1996). The limited presence of desiccation cracks, and overall purple color suggest deposition under oxidizing conditions (e.g. Turner, 1980; Miall, 1996; Retallack, 1997) with common subaerial exposure (e.g. Estaban and Klappa, 1983) while the development of calcareous nodules and bioturbation indicates pedogenic modification after deposition (e.g. Wright and Tucker, 1991; Retallack, 1997).

4.2. Yecua Fm

The up to 350 m-thick Upper Miocene Yecua Formation (Padula and Reyes, 1958) thins southward in the study area. Its presence in the western Chaco Plain (Villamontes region) is doubtful. Its overall deposits represent a short-lived marine incursion into the centre of the South American continent, probably made possible by the combination of global Upper Miocene sea level highstand and/or initial Andean loading of the Brazilian Shield. Hulka et al. (in press) postulated that

the marine transgression occurred from the north and was slightly older than the “Paranense” marine incursion from the south (Padula and Reyes, 1958). The contact of the Yecua Formation with the underlying Petaca Formation is sharp and unconformable (Tatarenda section, Figs. 2 and 3).

The Yecua Formation is composed mainly of calcareous sandstone, fossiliferous limestone, and varicolored mudstone (Suarez Soruco, 1999) and is divided into three major facies associations: (1) thin-bedded sandstone–mudstone couplets (Y1), (2) pebbly calcareous sandstone (Y2), and (3) fossiliferous varicolored mudstone (Y3; Table 3). Fig. 5 shows a typical stratigraphic profile and the three facies associations of the Yecua Formation at the particularly well-exposed Tatarenda section.

4.2.1. Y1. Laminated interbedded sandstone and mudstone

4.2.1.1. Description. This facies association consists dominantly of fine-grained, small-scale sandstone up to 1 m thick interbedded with red-brown mudstone. Its lithofacies are shown in Table 1. Small-scale symmetrical and cross-laminated ripples and erosional channels of 5 to 15 cm depth dominate the internal structures of the sand bodies; herringbone cross-stratification, flaser, wavy, and lenticular bedding, and convolute sedimentary structures are also present (Fig. 5B). Syndepositional channel-margin slumps occur occasionally. The identified lithofacies are flaser (Smf), wavy (Smv), laminated (Sml), herringbone (Smh), and ripple (Sr).

4.2.1.2. Interpretation. This facies association apparently formed under periodically reversing currents of slow to intermediate flow velocity in a mostly aggradational but locally erosional regime through broad and flat channels that collectively suggest a low-energy tidal environment (Hulka et al., in press). Laminated mudstones result from suspension fallout from standing water during slack-water conditions.

The presence of herringbone cross-bedding suggests the existence of tidal currents capable of producing bedform migration (Allen, 1980; Bristow, 1995). Upward decrease in grain size and vertical changes in bedforms indicate a decrease in flow velocity and sand supply, possibly related to the evolution of tidal flats.

4.2.2. Y2. Fossiliferous varicolored mudstone

4.2.2.1. Description. The fossiliferous varicolored mudstone facies is characterized by numerous repetitive, thickening- and coarsening-upward, 20–40 cm thick sets of laminated, reddish to greenish mudstone interbedded with calcareous, fine-grained, thin-bedded sandstone. These show parallel-stratified (Sh) and minor low-angle symmetrical cross-laminated ripples (Sr) and are interbedded with well-sorted, coarse- and very-coarse-grained shell hash coquinas (Shs; Fig. 5C). This facies association contains bivalves and foraminifera and abundant ostracode genera *Cyprideis* and *Heterocypris* (Hulka et al., in press). This facies association is well developed at the Abapó section (Fig. 2).

4.2.2.2. Interpretation. The internally continuous, thickening- and coarsening-upward mudstone–sandstone sets are likely related to minor periodic fluctuations in water depth, whereas the mudstone color variations suggest frequent changes between oxidizing and reducing conditions. The high variability in water depth and seafloor chemistry is consistent with the fossil record: Meisch (2000) describes species of the genus *Heterocypris* with variable salinity tolerance, mostly living in freshwater and brackish environment. Similarly, *Cyprideis* is a genus typical of meso- to polyhaline brackish environments although it also occurs in freshwater and marine environments. Only the planktonic foraminifera *Globigerinacea* indicates a marine environment. Overall, this facies association appears to have formed in a marginal to shallow marine setting.

Fig. 4. Stratigraphic profile of the Petaca Formation in Tatarenda section (No. 2 in Fig. 2) showing (A) depositional environments, (B) horizontally bedded pebbly sandstone of facies association P3, (C) polymictic pebbly conglomerate consisting of dominantly reworked pedogenic and minor non-pedogenic clasts of facies association P2, and (D) densely packed nodular calcrete horizon developed on sandy substrate of facies association P1.

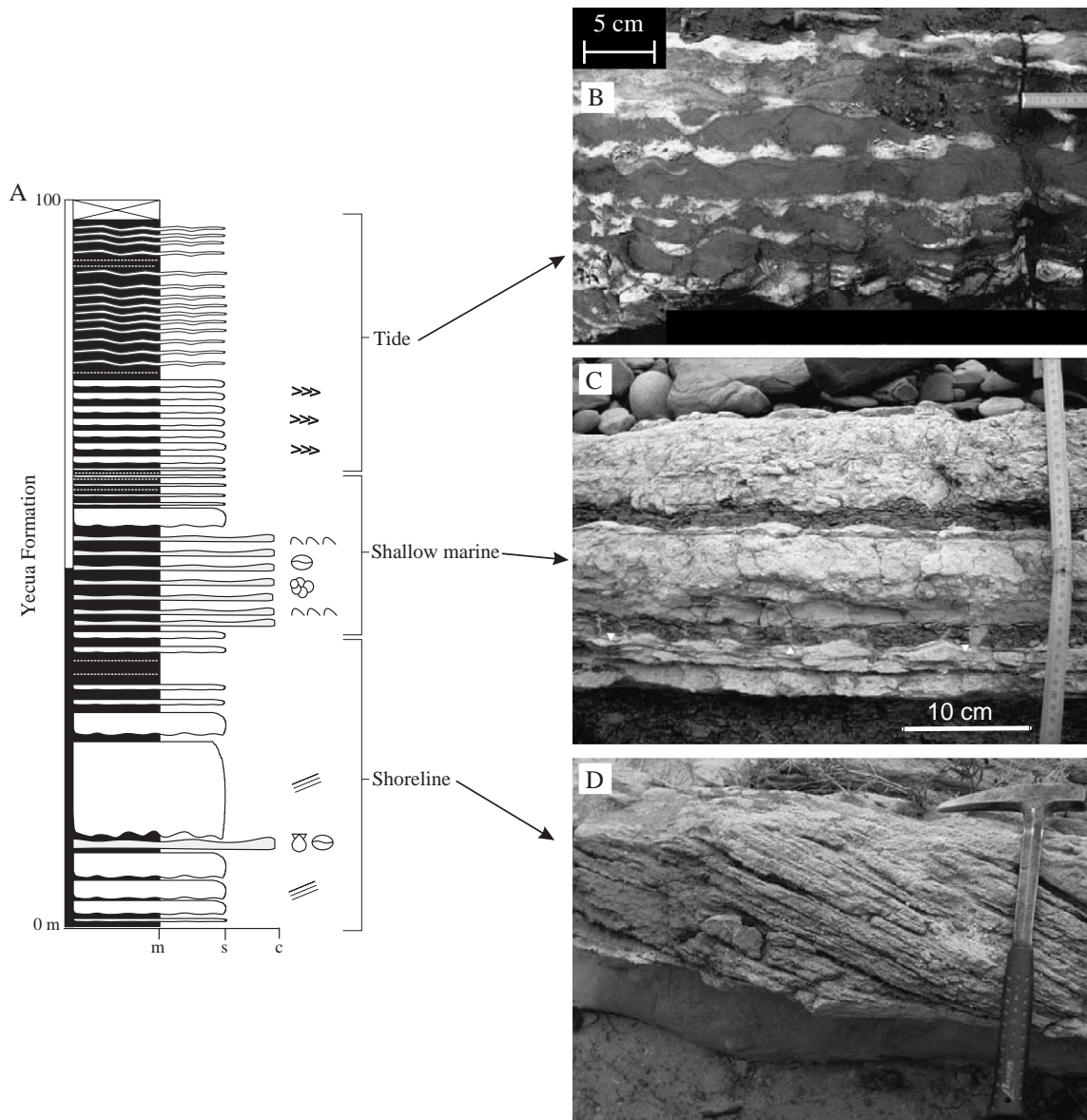


Fig. 5. Stratigraphic profile of the Yecua Formation in the Tatarenda section (No. 2 in Fig. 2) showing (A) depositional environments, (B) wavy to lenticular stratification in fine-grained sandstone and mudstone described as facies association Y1, (C) shell-hash dominated, interbedded sandstone, mudstone and mudcracks of facies association Y3, and (D) medium-scale, planar, cross-bedded coarse-grained quartzose sandstone of facies association Y2.

4.2.3. Y3. Calcareous sandstone

4.2.3.1. Description. The typical lithofacies character of this facies association consists of coarsening-upward, white, coarse- and very-coarse-grained, poorly sorted, calcareous, quartzose sandstone up to

30 cm thick and subordinate pebbly clasts. Common sedimentary structures include asymmetrical ripple cross-laminations (Sr) and well-developed low-angle planar-stratification (Sp) (Fig. 5C). Subordinate red and green, massive and bioturbated mudcracked mudstone also occur. This facies asso-

ciation reaches up to 30 m in thickness and is best developed at the Oquitas and Saipuru sections (Fig. 2).

4.2.3.2. Interpretation. This group of strata is indicative of a low- to mid-energy shoreline facies including a migrating foreshore and upper shoreface under an active wave regime (e.g. Einsele, 2000). The material is a mixture of coastal marine sediments and reworked sands, presumably delivered from a nearby delta complex (Hulka et al., in press). This interpretation is consistent with the occurrence of asymmetrical ripple cross-beds and low-angle planar structures and by the presence of bioturbation (Einsele, 2000). The coarsening-upward trend reflects seaward shoreline progradation.

4.3. Tariquia Fm

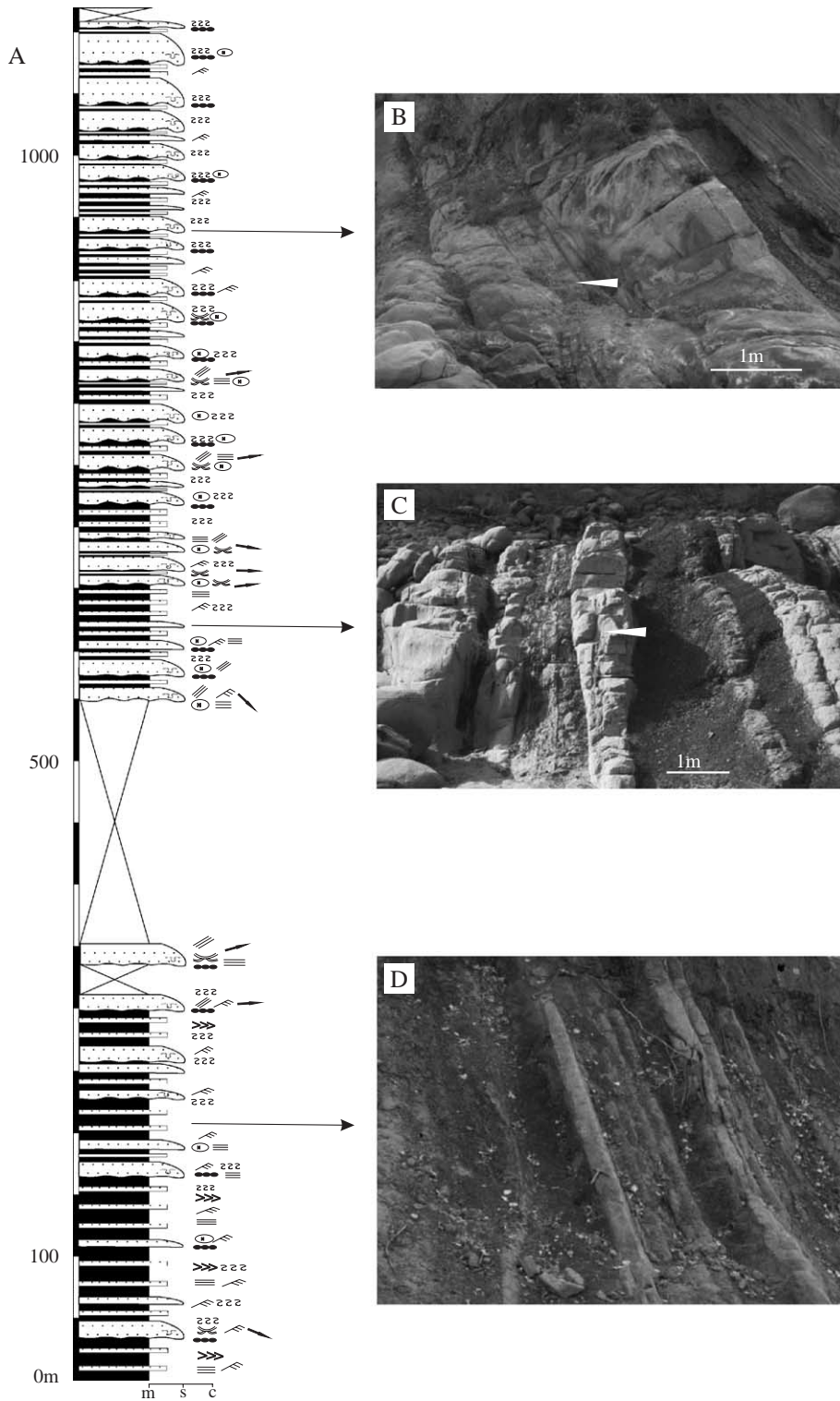
Strata of the widespread and well-exposed Tariquia Formation or Chaco Inferior (Russo, 1959; Ayaviri, 1964) consist of up to 4500 m of sandstone and mudstone. This formation overlies transitionally the marginal-marine Yecua Formation in the eastern and northern part of the study area and overlies unconformably the Petaca Formation in its southern part. The up to 600 m-thick lower Tariquia member is dominated by thick mudstone and subordinate sandstone, whereas the more than 3500 m-thick upper member is sandstone-dominated. Fig. 6 shows a characteristic profile and outcrop photographs of this formation at the Angosto del Pilcomayo section, ~4 km east of Villamontes (Fig. 2). Three facies associations are recognized in the Tariquia Formation: (1) thick-bedded sandstone (T1), (2) thin-bedded sandstone (T2), and (3) mudstone-dominated, interbedded mudstone and sandstone (T3; Table 3).

4.3.1. T1. Thick-bedded sandstone

4.3.1.1. Description. The thick-bedded sandstone facies association consists of 2-to-15 m-thick, light brown, light yellow, and light red, well sorted, medium- to very-fine-grained sandstone with abundant red intraformational pebble-sized mud chips (Ss) and occasionally reworked calcareous paleosol nodules. Individual beds are 1 to 20 m thick and show very little fining-upward tendencies (Fig. 6B), possibly due

to the lack of available grain size variability. The sandstone shows ribbon geometry, extend laterally for hundreds of meters, are moderately channelized, and shows sharp erosional bases (Miall, 1996; Fig. 7). Their degree of vertical stacking and lateral interconnectedness increases upsection. Grain size and sandstone proportion increase regionally westward. Outcrop observations document small- to medium-scale trough cross (St), planar (Sp), massive (Sm), horizontal (Sh), climbing- and ripple-cross (Sr) lithofacies (Miall, 1996). Channel (CH) and sandy bedforms (SB) are the common architectural elements. Limited plant fragments, occasional small-scale soft-sediment deformation, a variety of dewatering structures, and abundant trace fossils *Taenidium* disrupt the primary sedimentary fabrics. This facies association is incised into or grades upward into the interbedded mudstone and sandstone facies association.

4.3.1.2. Interpretation. The laterally extensive and erosive-based sandstone represent deposits of major mixed-load channels with fluctuating stream competence. The assemblage of channel (CH) and sandy bedforms (SB) architectural elements indicates a low-sinuosity channel morphology. The aggrading floodplain architecture, the dominance of vertically stacked channels, and the aggradation of SB in overbank deposits suggest a very limited channel migration tendency (e.g. Smith and Smith, 1980; Smith, 1983; Kirschbaum and McCabe, 1992; McCarthy et al., 1997; Makaske et al., 2002). The channel base experienced alternating scouring, bed-load transport, and deposition. In addition, this facies association is dominated by frequent crevassing and avulsion, which led to formation of new channels on the floodplain, while active channels were abandoned (e.g. Smith, 1986; Smith et al., 1989; Makaske et al., 2002). The abundant intraformational mudclasts and scours suggest erosion of significant amounts of cohesive mud of the overbank facies during bankfull flow. The ripple-cross laminations (Sr) occasionally found at the bed tops indicate gradual waning in flow and channel abandonment (Smith et al., 1989; Miall, 1996). Floodplain sedimentation, subaerial exposure and post-flood organic activity are indicated by soft-sediment deformation structures, climbing ripples, mud chips, desiccation cracks, and weakly developed paleosols (Miall, 1996).



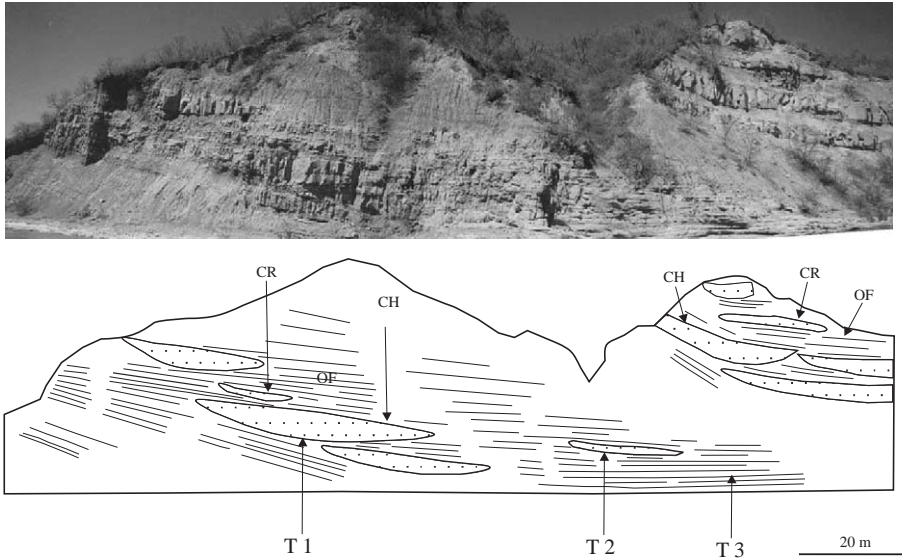


Fig. 7. Outcrop photomosaic and line drawing of the lower Tariquia Formation in Oquitas, (No. 6 in Fig. 2) showing the transition between facies associations T1, T2, and T3.

4.3.2. T2. Thin-bedded sandstone

4.3.2.1. Description. The thin-bedded FA consists dominantly of light brown to light yellow, well sorted, very fine- to medium-grained massive (Sm), trough- and ripple-cross-bedded (St, Sr), and horizontally bedded (Sh) sandstone which reaches 0.5–5 m thick and typically extends laterally for tens of meters (Fig. 6C). In this, they are significantly narrower than the previous facies association, but only moderately reduced in unit thickness (Fig. 7), resulting in an overall lower width-to-depth ratio. Bases of the sandstone show irregular, concave-up, erosional bounding surfaces and contain pebble-sized rip-up clasts of red mudstone (Se). Climbing ripples and ripple-cross bedding are common in the upper part of the thin-bedded sandstone. The upper boundaries are mostly flat and transitional to red mudstone, but occasionally sharp. Sandy bedforms (SB) are the common architectural element in this facies association. Fining- and coarsening-upward sequences, burrows, moderate to rare

plant remains, and incipient soil formation recognized by calcareous nodules and internal fabric reorganization are common. This facies association is incised into or grades into the interbedded mudstone and sandstone facies association.

4.3.2.2. Interpretation. We interpreted the thin-bedded sand bodies as deposits in mixed-load minor channels, such as crevasse channels with fluctuating stream power because the aforementioned processes generally occur in channels, are in proximity to major channel sandstone bodies, and show a concave-up channel geometry in cross section (Miall, 1996). Thickness and lateral extent of individual element groups indicate that the channels were shallow to moderately deep (~0.3–1 m). The presence of St, Sh, and Sr lithofacies suggest that deposition occurred largely in the upper flow regime. The fining- and coarsening-upward trends may result from changes in stream strength during deposition or gradual channel abandonment (Bristow, 1995; Miall, 1996). Climbing ripples and

Fig. 6. Stratigraphic profile of the Tariquia Formation in the Angosto del Pilcomayo section (No. 10 in Fig. 2) showing (A) an overall upsection increase in channel-fill sand bodies, (B) close-up view of multi-storey (arrow), thick-bedded, channel-fill sandstone of facies association T1, (C) ribbon-shaped, thin-bedded sandstone from minor crevasse channels of facies association T2 (arrow) interbedded with floodplain facies, and (D) interbedded sandstone and mudstone from floodplain facies of facies association T3.

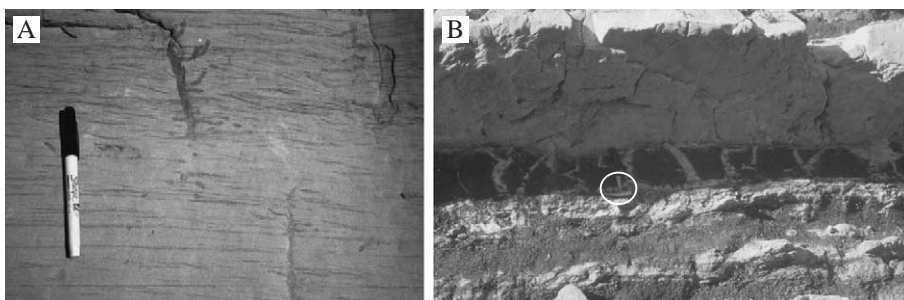


Fig. 8. Outcrop photographs of the Tariquia Formation showing (A) bioturbated (*Taenidium*) small-scale rippled fluvial sandstone of facies association T1, and, (B) well-developed mudcracks in floodplain sediments (T3). See hammer for scale (cycled).

ripple-cross-bedding in the upper fine-grained sections of individual channels indicates periodic channel reactivation, incision, and abandonment whereas abundant burrowed or mottled sandstone suggest periods of channel abandonment or partial emergence of sand bars between floods. Finally, the basal erosive surfaces indicate erosion by strong stream currents and a reduction in depositional rate.

4.3.3. T3. Interbedded mudstone and sandstone

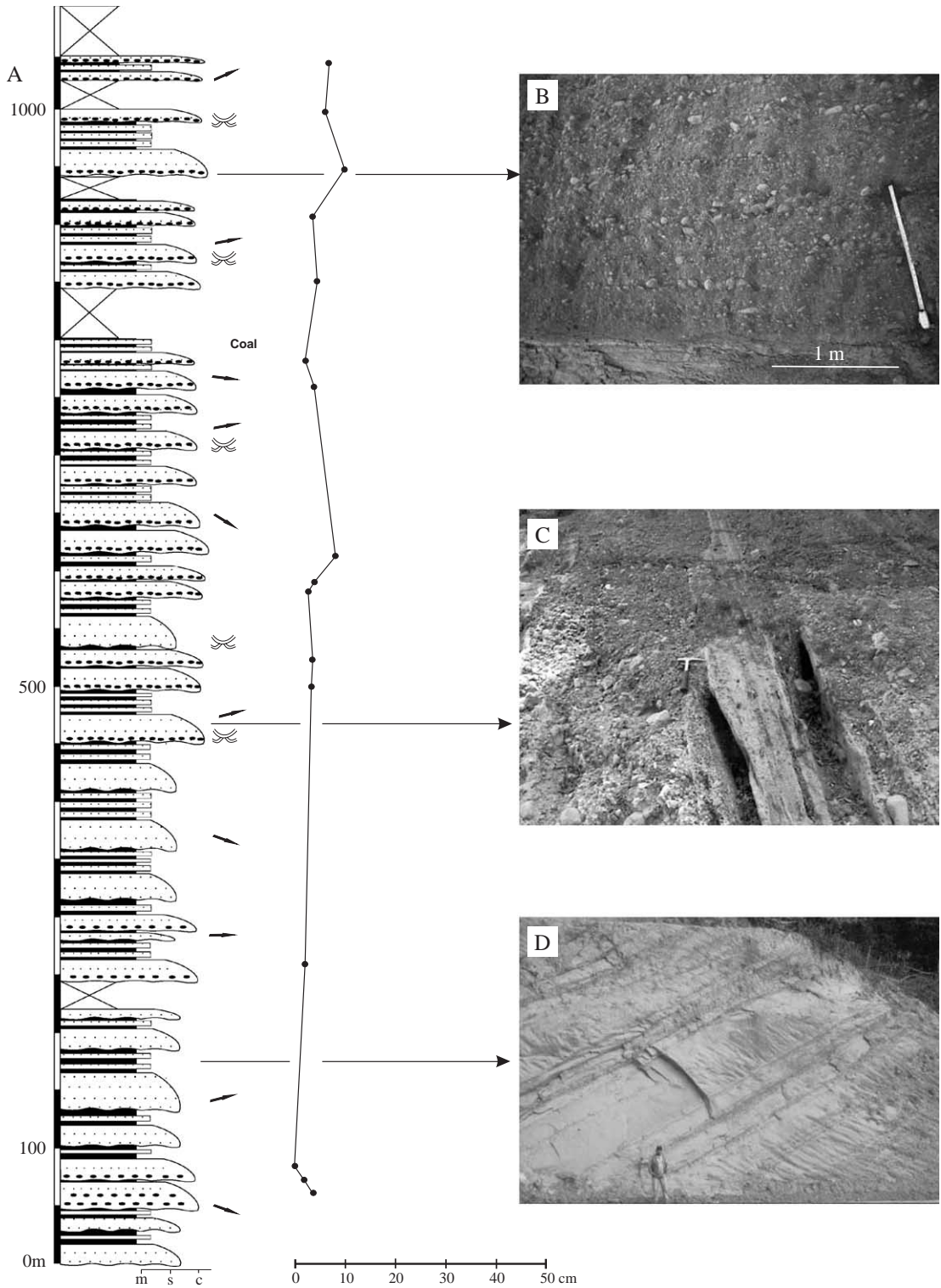
4.3.3.1. Description. Upsection changes in the frequency of the interbedded mudstone and sandstone facies association define the boundary between a mudstone-dominated lower Tariquia member (75%) and a sandstone-dominated upper Tariquia member (70%). Red to light-brown, fine- to medium-grained, fining- and coarsening-upward sandstone occurs in sheet and rarely lenticular geometries of 0.5 to 3 m thickness extending laterally for several hundred meters intimately interbedded with mudstone (Fig. 6D). The element groups mostly consist of massive (Sm), laminated (Sl), and ripple cross-bedded (Sr) stratifications. The facies architectural elements include laminated sand sheets (LS) and sandy bedforms (SB).

Red to chocolate-colored, laterally very extensive, horizontally laminated (Fl) or massive (Fm) mudstone separate the sand sheets. Rare, poorly developed nodular horizons in them indicate weakly developed paleosols. Abundant *Taenidium* trace fossils (Fig. 8A),

desiccation cracks (Fig. 8B), calcareous and rare ferruginous nodules in sand- and mudbodies disrupt and obliterate primary sedimentary structures to a high degree.

4.3.3.2. Interpretation. Strata of this FA are interpreted as overbank and floodplain deposits produced by the waning flow strength of sandy to muddy sheet-floods through crevasse splays or in standing floodplain water, respectively. In particular, sand bodies of lenticular shape represent crevasse splay and levee deposits by virtue of their proximity to major channels and occasionally observable coarsening-upward trends (e.g. Smith et al., 1989; Bridge, 1993; Ferrell, 2001) whereas SB elements and horizontal bedding surfaces probably represent products of distal splays and waning flow energy (Miall, 1996). The upward-coarsening and -thickening trends suggest minor phases of crevasse lobe migration into the floodplain (Ferrell, 2001), and fining-upward successions imply crevasse splay abandonment (Ghosh, 1987). Laminated mudstone (Fl) mark suspended-load deposition from low-velocity floods; they were frequently reworked by bioturbation and pedogenic processes, resulting in massive mudstone (Fm). Mudstone color, abundance of desiccation cracks, burrows, and calcareous nodules suggests well-drained or even partially emergent floodplains (Retallack, 1997; Mack et al., 2003) and substantial aerial exposure (McCarthy et al., 1997).

Fig. 9. Stratigraphic profile of the Guandacay Formation in the Emborozu section (No. 15 in Fig. 2) showing (A) an overall coarsening- to fining-upward sequence in maximum clast size within the gravel to cobble conglomerate, (B) close-up of fining-upward erosive channel conglomerate bodies of facies association G1; clasts are aligned subhorizontally, (C) close-up of fining-upward channelized sand bodies of facies association G2 (hammer for scale); stratigraphic top is to the right, (D) interbedded sandstone and sandy mudstone of facies association G3. Person is 1.8 m in height. Beds dip $\sim 40^\circ$ to the left.



4.4. Guandacay Fm

The transition from the Tariquia Formation to Guandacay Formation is conformable and defined by a transition from dominantly fine-grained sandstone to pebbly conglomerate. The Guandacay Formation (Jimenez-Miranda and Lopez-Murillo, 1971), earlier known as Chaco Superior (Ayaviri, 1967) was spectacularly exposed in 2003 in continuous roadcuts near Emborozu of southernmost Bolivia near the Argentina border (No. 15 in Fig. 2). These roadcuts allowed a complete new description of the lithology and architectural elements of this formation. It consists principally of pebble conglomerate and coarse-grained sandstone with minor mudstone and shows an overall coarsening- and thickening-upward sequence (Fig. 9). Grain size and conglomerate proportion increase regionally westward. The up to 1500 m-thick Guandacay Formation consists of three facies associations (Table 3): (1) granule to cobble conglomerate (G1),

(2) coarse-grained sandstone (G2), and (3) sand-dominated interbedded sandstone and mudstone (G3).

4.4.1. G1. Granule to cobble conglomerate

4.4.1.1. Description. Individual lithofacies types of the granule to cobble conglomerate facies association are summarized in Table 2, and a vertical type profile is shown in Fig. 9A. The facies association consists dominantly of organised, moderately to well sorted, polymict, mostly clast-supported (Gcd and Gco with minor Gh and Gt lithofacies) granule to cobble conglomerate (Fig. 9A). Architectural elements include gravelly bedform (GB) and poorly developed lateral accretion (LA). The conglomerate comprise rounded to well-rounded clasts of sandstones and quartzites showing imbrication and common normal grading. Flat, non-erosional to erosional bases bound the sheet-like or lenticular conglomerate bodies (Fig. 10). Individual beds reach up to 10 m in thickness and extend laterally for several tens to

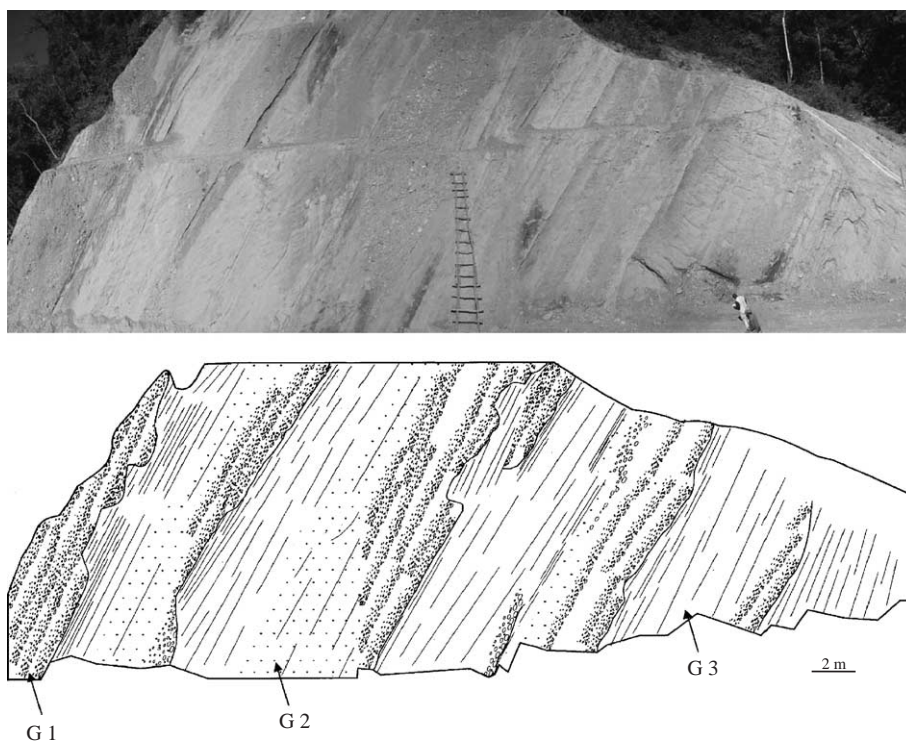


Fig. 10. Outcrop photomosaic and line drawing of the Guandacay Formation in Emborozu section, (No. 15 in Fig. 2) showing the transition of the facies associations G1, G2, and G3.

hundreds of meters. This facies association shows upsection-coarsening trends.

4.4.1.2. Interpretation. The dominance of organised fabrics and moderately to well-sorted clasts in this facies assemblage suggests deposition by persistent high-energy tractional processes dominated by stream flows in low-sinuosity, gravel-dominated channels in which transportation occurred largely by bedload and deposition occurred under waning flow conditions. This interpretation is supported by the presence of erosional surfaces, imbrication, and the dominance of Gco over Gcd lithofacies. The disorganised lithofacies (Gcd) usually represents rapid deposition from high-concentration sediment dispersions. In contrast, the organized lithofacies (Gco) demonstrates deposition in gravel sheets or longitudinal bars (GB) (e.g. Boothroyd and Ashley, 1975; Todd, 1989; Brierley et al., 1993). The observed occasional inverse grading could be due to limited grain interaction in a restricted, highly concentrated bedload or traction carpet (Todd, 1989). The cyclic fining-upward sequences indicate waning flood flow velocities of individual high-water events.

4.4.2. G2. Coarse-grained sandstone

4.4.2.1. Description. The coarse-grained sandstone facies assemblage includes medium- to very coarse-grained, well to moderately sorted, subrounded to subangular, light brown to light gray pebbly sandstone (Fig. 9C), interbedded with conglomerate of G1. The common lithofacies in the sandstone bodies consist of St, Sp, and Sh lithofacies with occasional stringers of pebble outlining low-angle cross-bedding (Gp). Sandbodies contain little clay matrix. This facies association shows fining-upward sequences, with individual bed decimeters to several meters thick and laterally discontinuous (Fig. 10). In cross section, the beds show poorly developed lateral accretion surfaces with occasional small-scale basal scour surfaces (Ss).

4.4.2.2. Interpretation. This facies association is produced by sandy stream floods in the waning stages of a major flow events in channels. The lenticular and tabular geometries and their fining-upward sequences indicate individual stream floods comprised of channel processes (CH) and limited to poorly developed lateral

accretion (LA) elements. Sandbars were deposited in shallow scoured channels just after peak flood flow (e.g. Miall, 1996; Gupta, 1999). The cyclic trend and vertical stacking of the fining-upward units in this facies association indicate repeated fluctuations in flow velocity. The pebble content of the sandstone shows that bedload rolling of clasts took place at the same time as fall-out of sand loads (Miall, 1996; Gupta, 1999). The Gp lithofacies suggests gravel deposition from longitudinal bars (Boothroyd and Ashley, 1975) whereas the paucity of internal bounding surfaces within the fining-upward strata suggests rapid deposition. The large-scale St lithofacies may represent channel pools or slightly elevated surfaces within broad channels. The presence of slip-faces in Sp and their lateral accretion pattern suggest deposition in simple bars (Todd, 1996). The St and Sh sandbodies were probably deposited in upper-flow regime plane beds and subaqueous sand dunes.

4.4.3. G3. Interbedded sandstone and mudstone (sandstone-dominated)

4.4.3.1. Description. The interbedded sandstone and mudstone facies association is sandstone-dominated and comprises interbedded light brown to light-red sheet sandstone (70%) and red to chocolate sandy mudstone (30%) (Fig. 9D). The medium- to coarse-grained sandstone consists of Sl, Sm, and Sr lithofacies. Bodies are laterally continuous for several tens to hundreds of meters and reach up to 50 m in thickness. The subordinate, centimeter-thick mudstone is massive (Fm) or laminated (Fl). Poorly preserved bioturbation and very thin beds of low-rank coal are occasionally present. This facies association is closely associated with G1. This facies association also occurs in the Emborozu Formation (Table 3).

4.4.3.2. Interpretation. Grain size, sheet-like geometry, and lack of distinct channelization structures argue for floodplain deposits (Fig. 10). The few-centimeter-thick (Fm) lithofacies probably represents deposition from low-energy flows or from standing pools of water during channel abandonment (e.g. Miall, 1996). The sheet and laterally continuous geometry, coupled with characteristic lamination (Fl), are evidence for slow-flowing or standing water (e.g. Miall, 1996; Bridge,

2003). Poorly developed pedogenic suggest constant and continuous overbank flooding. The occasional presence of coal beds (as opposed to calcareous mudstone) suggests the presence of peat swamps undergoing rapid plant accumulation under a humid paleoclimate (e.g. McCabe, 1984), possibly further supported by the absence of mudcracks (e.g. Smoot, 1983).

4.5. Emborozu Fm

The Pliocene–Quaternary, up to 2000 m-thick Emborozu Formation (Ayaviri, 1967) marks the proximal wedge-top foreland system in the SZ (Uba and Heubeck, 2003). Its base is a regional angular unconformity (Gubbels et al., 1993; Dunn et al., 1995; Moretti et al., 1996; Echavarría et al., 2003). The formation consists of a coarsening-upward sequence of cobble–boulder conglomerate (Fig. 11A) with interbedded subordinate, thinning-upward red sandstone and mudstone. Furthermore, a gradual upsection increase in clast size is observed. The strata of this formation show syndepositional growth structures in seismic sections (Gubbels et al., 1993; Dunn et al., 1995; Moretti et al., 1996; Echavarría et al., 2003; Uba et al., submitted for publication). Three facies associations are distinguished: (1) cobble–boulder conglomerate (E1), (2) sheet sandstone (E2), and (3) interbedded sandstone and sandy mudstone (Table 3), the latter previously described as G3 in the Guandacay Formation.

4.5.1. E1. Cobble to boulder conglomerate

4.5.1.1. *Description.* Clasts of the cobble–boulder conglomerate facies association form crude clusters along bedding, reach up to 153 cm in diameter, are subangular to well rounded, and moderately sorted. The clast-size distribution is polymodal and shows inverse to normal grading (Fig. 11B); imbrications are moderately to poorly developed (Fig. 11C). The bases of the conglomerate beds are sharply erosive to underlying sandstone and sandy mudstone. Individual

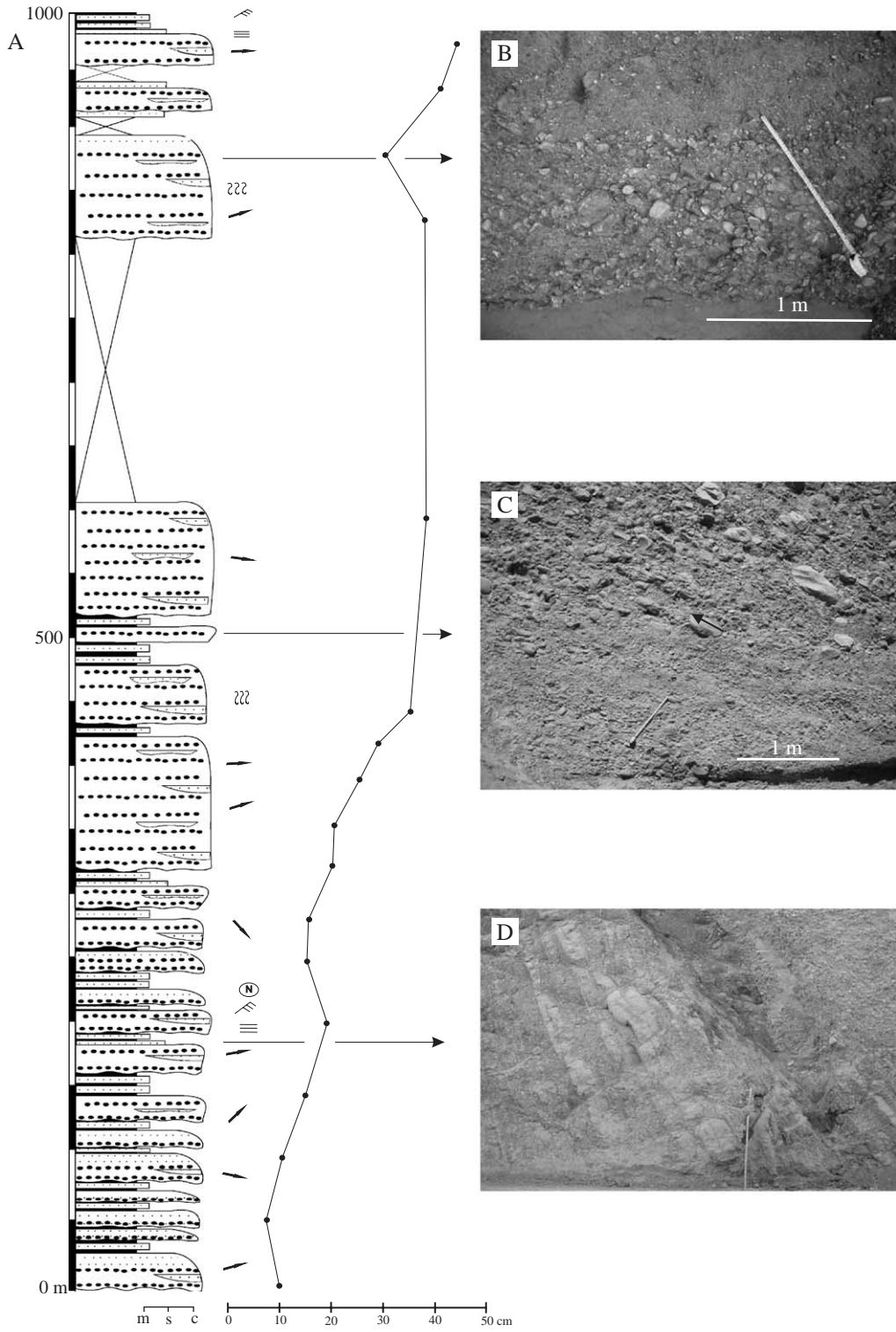
beds show sheet-like to lenticular geometries, laterally extending for several tens of meters (Fig. 12). The conglomerate consist of disorganized matrix-supported (Gmd), disorganized (Gcd), organized (Gco) and scour surfaces (Ss) lithofacies within a very coarse-grained sand matrix (Table 1). The reorganized architectural elements are gravel bed (GB), channel (CH), and poorly to limited lateral accretion (LA).

4.5.1.2. *Interpretation.* The cobble-to-boulder conglomerate facies association is interpreted as resulting from high-energy streamfloods equivalent to those produced by gravel-laden streams in poorly to well confined channels (e.g. Maizels, 1989; Brierley et al., 1993; Ridgway and DeCelles, 1993; Blair, 1999), consistent with the clast-supported fabric, basal erosion surfaces, weakly to moderately developed clast imbrications, and lenticular and cross-stratification. The beds geometry represents gravel sheets or low-relief longitudinal bars (Boothroyd and Ashley, 1975; Todd, 1989). The organized clast-supported conglomerate (Gco) with moderately developed imbrications may be a result of incised-channel gravel bedload sedimentation under accreting low-to waning-energy flows (Jo et al., 1997; Blair, 1999). This is supported by thick vertical-accreting conglomeratic beds and erosive surfaces. In contrast, the poorly developed and disorganised bedforms (Gcd and Gmd) suggest high sedimentation fallout rates and/or shallow flow depth (e.g., Jo et al., 1997; Blair, 1999). The good rounding of the clasts was probably a result of abrasion during cyclic sediment transport and storage. The trough cross-bedded sand bodies represent deposits in channels, which may have developed under waning flow strength (Boothroyd and Ashley, 1975).

4.5.2. E2. Sheet sandstone

4.5.2.1. *Description.* The sheet sandstone facies association consists of light brown to light-red, coarse to very coarse-grained, well sorted sandstone (ca. 80%)

Fig. 11. Stratigraphic profile of the Emborozu Fomation in its type Emborozu section (No. 15 in Fig. 2) showing (A) an overall coarsening-upward sequence in maximum clast size within the cobble-dominated conglomerate, (B) close-up of fining-upward channel conglomerate bodies showing erosive lower contact of facies association E1, (C) close-up of occasional inversely graded and imbricated channelized conglomerate of facies association E1, paleoflow to the left (arrow) stratigraphic top to the right, and (D) channelized sandstone with floodplain deposited sandstone and sandy mudstone of facies association E2 and G3. Person is 1.8 m in height.



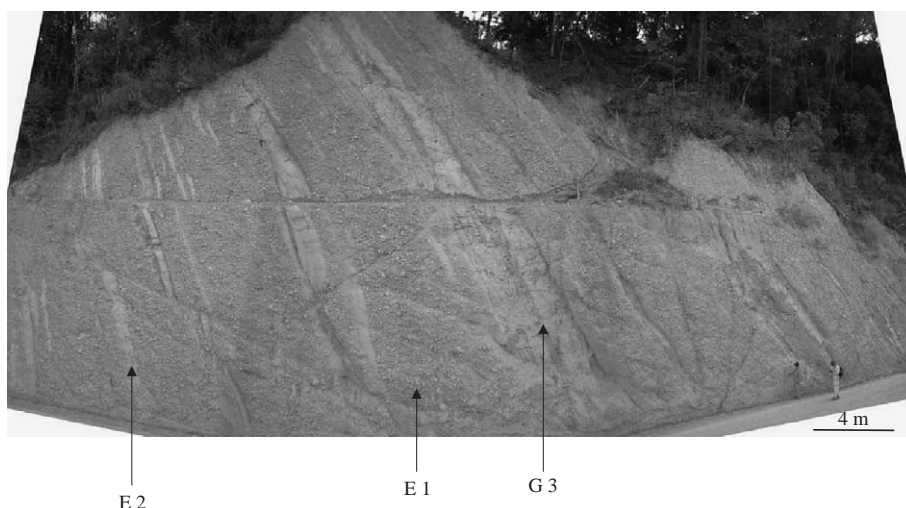


Fig. 12. Outcrop photomosaic of the Emborozu Formation in Emborozu section, (No. 15 in Fig. 2) showing laterally accreting, channelized sandstone and the facies associations E1, E2, and G3.

with minor conglomerate stringers (ca. 20%). Individual beds are fining-upward, ~2–6 m thick, sheet-like to lenticular in cross section, laterally continuous for tens of meters (Fig. 11C) but occasionally laterally discontinuously and with a flat to gradational base. The sandstone shows horizontal (Sh), moderately to poorly developed (St), planar (Sp), and low- to medium-scale scour fill (Ss) lithofacies with limited lateral variability. Architectural elements include channel (CH), sandy bedform (SB), and poorly preserved lateral accretion (LA). Stringers of organized (Gco) clast-supported, conglomerate units are subordinately present. These very thin pebbly conglomerate beds are poorly imbricated. This facies association grades upward into the interbedded sandstone and sandy mudstone facies association (Fig. 12).

4.5.2.2. Interpretation. The sheet and lenticular geometry combined with the fining-upward grain size indicate a bar architecture, thereby suggesting deposition by sandy sheet floods and stream flows in poorly confined channels. Rapid deposition by flash and sheet floods in a channel-and-bar pattern is indicated by lack of internal bounding surfaces in the fining-upward sequence and the laterally continuous bed geometry. The trough cross-bedded lithofacies (St) and the poorly developed LA elements may represent cut-and-fill or isolated shallow channels (Miall, 1985)

and vertical aggradation. Planar cross-stratification (Sp) may represent bars (Todd, 1996; Bridge, 2003). The discontinuous lateral extent and the lack of cosets suggests occasional progradation of the bar margin (e.g. Crews and Ethridge, 1993) during waning streamflow strength. The conglomerate stringers represent diffuse gravel or channel lag sheets (e.g. Nemeč and Postma, 1993).

5. Fluvial system patterns

The vertical transition from the Upper Miocene Tariquia Formation through the Guandacay Formation to the capping Emborozu Formation reflects a marked change in the fluvial architecture (Fig. 13). The fluvial patterns are characterized by a coarsening- and thickening-upward trend, and a net upsection increase in the average number, size and connectedness of channels and changes in the channel type from single- to multi-storey and to multilateral channels along with an overall decrease in the proportion of overbank deposits (Fig. 13). Regionally, the proportion of overbank sediments increases to the east, where the sediments consist of dominantly mudstone and thinly bedded sandstone. The average grain size and proportion of sandstone in outcrop increases upsection and westward.

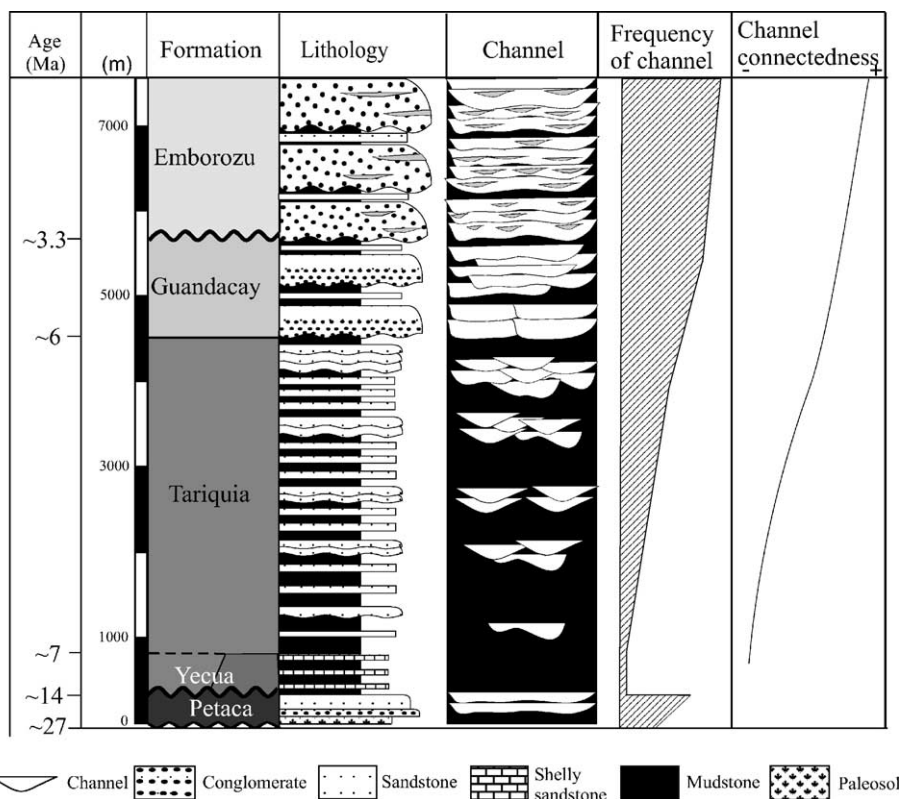


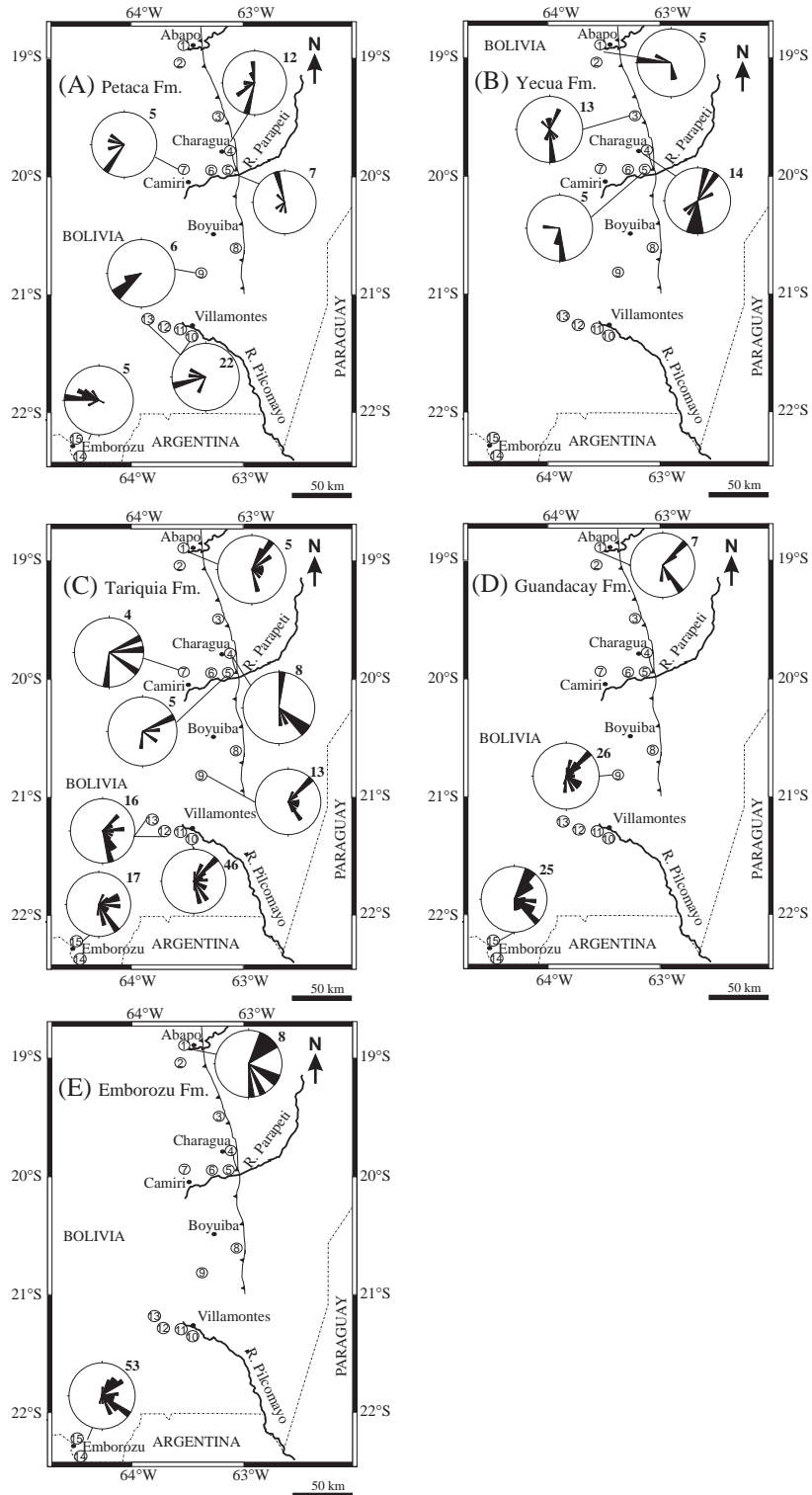
Fig. 13. Schematic changes in the depositional architecture of the Neogene Chaco foreland basin fill, based on lithofacies and architectural element assemblages.

Paleocurrent analyse of Neogene strata in the study area (Fig. 14A-E) indicate that basin sedimentation underwent two significant changes in principal direction of sediment transport. The principal flow and sediment transport direction in the Petaca Formation was to the west and southwest, indicating an easterly sediment source on the Brazilian Shield. Paleoflow directions in the Yecua Formation show polymodal patterns of transitional and marginal marine environments with an average flow direction to the southeast, thereby indicating a paleoflow longitudinal to the orogenic front. In the fluvial Tariquia Formation, a radial northeast-through-southeast paleocurrent pattern reflects a transverse system with respect to the deformation front, hence, a westerly source area. The paleocurrent dispersion patterns of the overlying Guandacay and Emborozu formations essentially maintain the same radial northeast-through-southeast pattern, indicating continued flow transverse to the deformation front.

6. Depositional models

The various facies and architectural features of the five Neogene formations in the SZ and CP can be integrated in depositional models (Fig. 15). Our work indicates that three distinct palaeoenvironmental settings characterized the Subandean Zone in the Neogene: (1) long periods of non-deposition, extensive soil formation, and extensive recycling in a braided fluvial setting during Petaca time; (2) marginal, shallow marine, and tidal environments during Yecua time; and (3) fluvial megafans of the Tariquia, Guandacay, and Emborozu Formations.

Calcretes in the Petaca Formation (Fig. 15A) represent long intervals of basin stability because the study area was starved of sediment. The crudely developed, shallowly channelized sandstone bodies of the Petaca Formation and the presence of reworked pedogenic conglomerate point to extensive recycling episodes in ephemeral short, braided



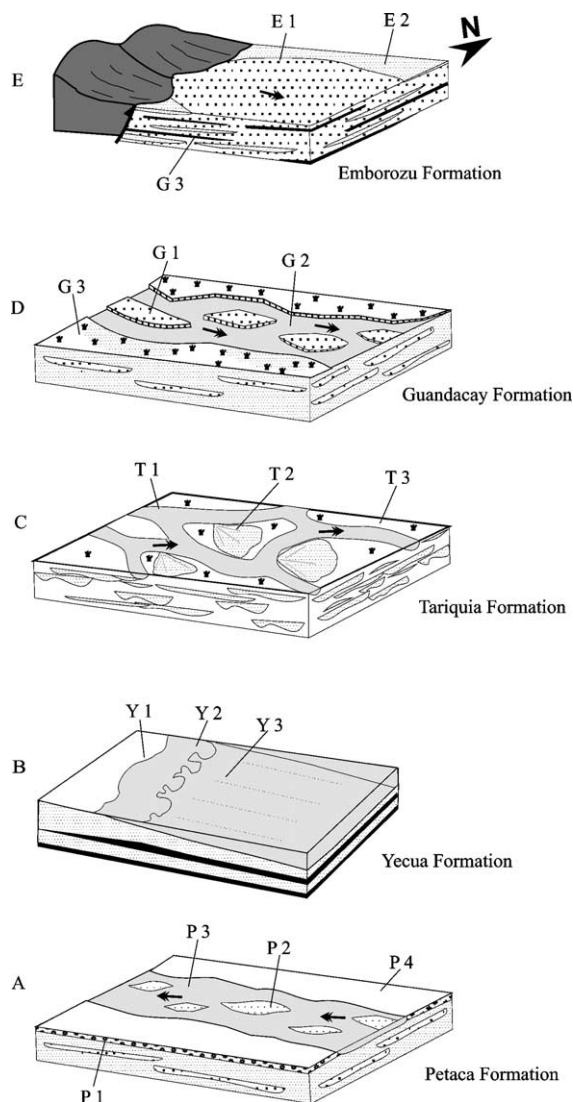


Fig. 15. Schematic block diagrams illustrating individual facies associations, their spatial relationship to each other, and depositional models for the five Neogene formations of the Subandean Zone and Chaco Plain.

streams of low lateral stability. Alternatively, but less likely, the compositional homogeneity of the reworked conglomerate could be due to local intrabasin paleohighs from which pedogenic conglomerate were eroded in large quantities. Khadkikar et al.

(2000) documented similar processes in the Chinji Formation, Pakistan.

The numerous cycles of sandstone interbedded with fossiliferous, laminated mudstone in the Yecua strata record several short-lived Upper Miocene marine trans- and regressions in the SZ and CP. Freshwater and shallow marine environments alternated depending on relative sea level and degree of tidal influence (Fig. 14B). These shallow marine sediments are well developed only in the northern part of the study area (e.g., Abápo and Tatarenda sections; Fig. 2), and the presence of the Yecua time-equivalent rocks south of Iguamirante section (Fig. 2) is debatable. Possibly, strata assigned to the lower Tariquia Formation in the south (e.g., Angosto del Pilcomayo) could be time-equivalent to the Yecua Formation (Echavarría et al., 2003). However, lithostratigraphic and facies arguments will not conclusively resolve this question, which highlights the general need for better chrono- and magnetostratigraphic constraints in the Chaco basin.

During Tariquia time, sediments aggraded rapidly on a subsiding floodplain, which was traversed by a network of low-gradient, well-defined channel networks separated by interfluvial areas of ponded areas (Fig. 14C). These characterize the Tariquia Formation as a high sediment-load anastomosing fluvial system, comparable in sedimentary facies and fluvial architecture to well-documented Recent systems from Colombia, Australia, and Canada (e.g. Smith and Smith, 1980; Rust, 1981; Smith, 1986; Makaske et al., 2002; Bridge, 2003; Tooth and Nanson, 2004). This interpretation is consistent with the high degree of channel interconnectedness, thick floodplain deposits, vertical aggradation, and the general lack of lateral channel migration. The coarsening-upwards sandstone bodies imply progradation of crevasse splays onto the flood-basin during flooding.

The Tariquia anastomosing river system was a long-lived, highly dynamic fluvial system with frequent crevasse and avulsion due to flooding and channel abandonment. Crevasse represents an important process to compensate for channel aggradation (Smith et al., 1989). The lack of lateral channel migration

Fig. 14. Aggregated paleocurrent data for the Chaco foreland basin: (A) for the Petaca Formation; (B) for the Yecua Formation; (C) for the Tariquia Formation; (D) for the Guandacay Formation; (E) for the Emborozu Formation. Rose diagrams represent paleocurrents, subscripts indicate the number of paleocurrent measurements. Thick fault line represents the mandeyepecua fault.

points to significant channel stability, vertical aggradation, and more-or-less straight channel geometry. In contrast, the frequent crevassing and avulsion also indicate channel instability, which could be due to lack of protective vegetation and high stream competence, as observed in modern ephemeral anastomosing streams (e.g. Rust, 1981; Brierley et al., 1993; Tooth and Nanson, 2004). The vertical stacking of sand bodies could be due to aggradation with minor shifting of channel bars associated with channel switching (e.g. Bridge, 1993). Overall, the Tariquia fluvial system experienced fluctuating but generally high depositional rates. The weakly developed paleosols may reflect a high floodplain aggradation rate (e.g. Kraus, 2002; Bridge, 2003). The high degree of bioturbation by *Taenidium* in the channels and floodplains, however, points to prolonged periods of more-or-less constant and moderate sedimentation rates between flooding events (Buatois et al., 2004).

The proximal, gravelly, braided streams of Guandacay time probably developed on large alluvial fans (Fig. 15D). The sharp basal contacts of individual conglomerate beds and the presence of thick and well preserved floodplains point to channel cutting and avulsion, whereas the poorly developed lateral accreting structures indicate low degree lateral migration and hence occasional channel instability. The low- to medium-scale sedimentary structures and thin- to medium-thickness bed sets in the Guandacay Formation indicate that channel depth was commonly on the order of a few meters or less. The thin coal beds testify to the former presence of vegetation, and therefore, a relatively humid paleoclimate.

During Emborozu time, high-energy stream flows deposited cobble to boulder conglomerate on proximal fluvial fans (Fig. 15E). The lack of ribbon sands suggests that channels experienced limited lateral migration. Furthermore, the Emborozu strata commonly show floodplain facies abruptly overlain by channel-deposited conglomerate. This is an indication of channel avulsion, similar to the pattern of the Paleogene Camargo Formation of Bolivia or the modern Kosi River of northern India (Sinha and Friend, 1994; DeCelles and Cavazza, 1999; Horton and DeCelles, 2001). The presence of substantial floodplain facies in this system distinguishes the Emborozu Formation from deposits of smaller alluvial fans (e.g. Clemente and Perez-Arlucea, 1993; Crews and

Ethridge, 1993; Blair, 1999). The occasional occurrence of laterally accreting sand bodies suggest deposits by adjacent distributary or incised channels, present in the modern Rio Pilcomayo (of the study area) or in Death Valley, California (Blair, 1999; Horton and DeCelles, 2001). The channel-fill pattern, poorly to moderately preserved small-scale sedimentary structures, and the thickness of the individual conglomerate beds in the Emborozu Formation indicate a flow depth of generally less than 2 m.

The Tariquia, Guandacay, and Emborozu strata show an overall upsection coarsening- and thickening-upward trend, coupled with upsection increase in average grain/clast size, distinct change in amount and size of channels, and decrease in the proportion of fine-grained floodplain sediments. Following other authors, we attribute these changes to the progradation of large fan lobes into the foreland basin (e.g. Clemente and Perez-Arlucea, 1993; Crews and Ethridge, 1993; DeCelles and Cavazza, 1999; Horton and DeCelles, 2001), representing distal through proximal fluvial megafan environments. Comparable modern and ancient analogues of similar fluvial architecture include the Kosi in India, the Ham Fork Conglomerate Member of the Evanston Formation in the Cordilleran Western Interior foreland basin, northwestern Wyoming, and the Camargo Formation of the central Bolivian Andes (Wells and Dorr, 1987; Sinha and Friend, 1994; DeCelles and Cavazza, 1999; Horton and DeCelles, 2001). DeCelles and Cavazza (1999) characterised fluvial megafans as a large, fan-shaped bodies of sediments deposited by a laterally mobile streams emanating from an outlet of a topographic front. They commonly form in proximal positions of non-marine foreland basins where confined, antecedent major rivers exit the fold-and-thrust belts and drain onto the unconfined floodplain (Wells and Dorr, 1987; Sinha and Friend, 1994; DeCelles and Cavazza, 1999; Horton and DeCelles, 2001), thereby radially depositing large volumes of sediment.

7. Controls on stratigraphic architecture

7.1. Climate

We used combinations of fauna and flora, paleosols, specific facies elements and depositional sys-

tems, coal, rip-up clasts, and the sand-to-mud ratio as relative indicators of paleoclimate (Smoot, 1983; Stear, 1985; Miall, 1996; Khadkikar et al., 2000). Fig. 16 lists indicators that allow us to conclude that a climate shift from arid to humid condition occurred in southern Bolivia during uppermost Tariquia time. The shift in climate in the study area is consistent with an arid-to-humid climate shift in northwestern Argentina (Hernandez et al., 1996; Starck and Anzótegui, 2001; Kleinert and Strecker, 2001).

We attribute the climate change in the study area to spatial (west–east) variation in climate rather than an abrupt temporal climate change. The semi-arid to arid climate during the deposition of Petaca and Yecua formations may reflect aridification due to major global and regional climate effect (e.g. Jordan et al., 1997). We attribute the Upper Miocene or Pliocene (?) climate shift of the Upper Tariquia Formation in the Chaco foreland basin to the creation of an orographic barrier to the west after the Andean range had attained sufficient elevation, creating a rain shadow to the west and capturing Atlantic moisture. Rain shadow effects due to spatial climate change in Argentina’s central Andes has been postulated by many researchers (e.g. Hernandez et al., 1996; Starck and Anzótegui, 2001; Kleinert and Strecker, 2001) but has not been demonstrated in the Bolivian SZ and CP. However, in northwest

Argentina, Hernandez et al. (1996) and Starck and Anzótegui (2001) postulated an Upper Miocene age for this spatial shift in climate while Kleinert and Strecker (2001) estimated ~5 Ma in age.

Climate change affects sediment supply, which in turn influences fluvial architecture, local drainage and floodplain stability. A shift toward higher humidity and precipitation causes net precipitation to exceed net evaporation, higher stream competency, efficient erosion, and higher sediment transport into the basin. The upper Tariquia Formation reflects this shift in climate by an upsection increase in average sandbody thickness, higher sediment-transport capacity, and larger channel widths.

7.2. Tectonics

The regional large-scale changes in sediment supply, fluvial pattern and facies architecture of the Neogene sequences were principally controlled by geodynamic processes associated with the Upper Miocene structural development of the Andes and the plate-tectonic interactions between the Nazca Plate and the western margin of the South American Plate. These processes are observed in the depositional systems and the general basin compartmentalization. Lithofacies, paleocurrent patterns, and fluvial architecture allow us to suggest that the Neogene

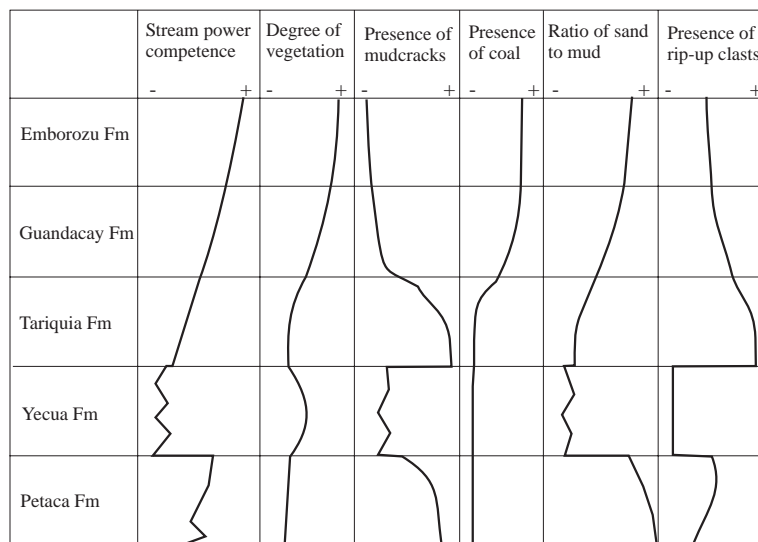


Fig. 16. Upsection stratigraphic variations in litho- and pedofacies climate indicators as in the study area.

sedimentation in the Chaco foreland basin may have been influenced by major deformation episodes of Upper Miocene age.

Calcretes of the Petaca Formation probably formed over a long interval of basin stability (see Gubbels et al., 1993) and indicates that the study area experienced a period of limited or non-sedimentation under arid conditions between the Upper Cretaceous (?) and the Upper Oligocene, over a period as long as 30 Ma. Therefore, the Petaca Formation represents a pre-foreland sequence and forms a regional drape throughout the basin. Reworked conglomeratic and sandstone beds of the upper Petaca Formation may reflect a forebulge–backbulge depocenter sequence (Fig. 17A), which, however, could not be fully ascertained in our work. We speculate that marginal marine facies of the overlying Yecua Formation may reflect the earliest recognizable

influence of Andean deformation in the Chaco foreland basin. By that time, around 10 Ma ago, the deformation front had entered the Subandean Zone (Sempere et al., 1990; Marshall and Sempere, 1991; Gubbels et al., 1993; Dunn et al., 1995; Kley et al., 1999; Echavarría et al., 2003) that led to deposition of Yecua distal foreland strata.

The upward-coarsening and -thickening trend, increase in channel size and upward low proportion of overbank deposits, coupled with avulsion channel behavior, and overall reversal in sediment dispersal direction in the Tariquia and Guandacay formations demonstrates eastward propagation of the Chaco depositional system and continuous deposition of foreland sequence sediments (Fig. 17B). Propagation of depositional systems likely reflects eastward propagation of the fold-and-thrust belt during the Upper Neogene (e.g. Moretti et al., 1996; Kley et al., 1999;

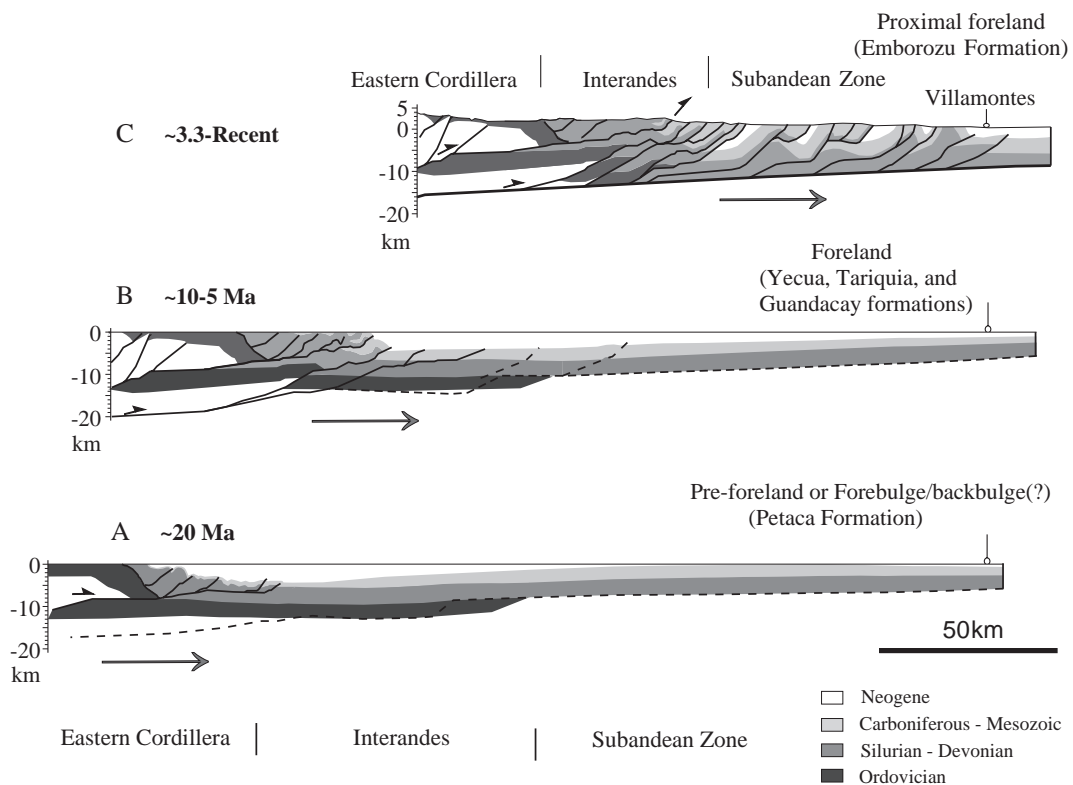


Fig. 17. Schematic diagram of structural cross sections of the Andes modified after Dunn et al. (1995) and Kley (1999) showing Neogene basin development in response to Andean tectonism. (A) Petaca, Formation was deposited as pre-foreland and/or forebulge–backbulge depocenter. (B) Yecua, Tariquia and Guandacay formations suggest foreland deposition. (C) The Emborozu Formation suggest foreland deposition proximal to topographic front.

Echavarría et al., 2003). A dramatically growing sediment supply during Tariquia and Guandacay time, based on their substantial thickness, shows that the foredeep depocenter migrated into the study area and increased accommodation space. Changes in the fluvial architecture prior to deposition of the Emborozu Formation immediately ahead of a migrating topographic front may have been due to renewed thrusting at ~3.3 Ma-Recent (Moretti et al., 1996), as evidenced by the numerous syn-sedimentary growth structures and boulder-sized conglomerate. We interpret the Emborozu Formation as a deposit in the proximal foreland system (Fig. 17C). This renewed onset of thrusting caused rapid uplift, sedimentary recycling and deposition of a cobble–boulder-dominated siliciclastic wedge. The upward-coarsening trend and rapid downstream changes in average clast size indicate that the conglomerates were trapped in a rapidly subsiding basin. Steel et al. (1977) and Crews and Ethridge (1993) documented similar numerous coarsening- and thickening-upward successions attributable to tectonic activities.

The coarsening- and thickening-upward foreland sequence (Yecua, Tariquia, Guandacay, and Emborozu formations) of the Chaco foreland basin show comparable variations in fluvial pattern and tectonic drivers on the migration of the depositional systems in time as the Upper Permian–Lower Triassic Karoo foreland basin, South Africa and the Pliocene–Pleistocene Himalayan foreland basin, India (Catuneanu and Elango, 2001; Kumar et al., 2003).

8. Conclusions

Facies association, lithofacies, and architectural elements of the Neogene sedimentary successions in the Chaco basin indicate three depositional settings. They commenced with Upper Oligocene, easterly sourced ephemeral braided streams and well-developed calcrete paleosols of the Petaca Formation representing widespread non-/low deposition. A second depositional setting is represented by the shallow marine, tidal, and shoreline-deposited Yecua Formation, which heralded the influence of Andean deformation in the study area in the Upper Miocene. Finally, the overall coarsening- and thickening-upward, distal through proximal fluvial megafan

sequence of the Tariquia, Guandacay, and Emborozu formations composed of deposits from anastomosing and braided streams and fluvial fan settings characterize the Chaco foreland basin. The fluvial megafan sequence shows common features such as reversal of drainage pattern, increase in channel abandonment, frequency of channel avulsion, thick floodplain deposits, and large-scale fluvial architecture, expressed by the quasi-continuous eastward progradation of large-scale, coarse-grained sediment lobes.

The transition from the lower Tariquia to the upper Tariquia Formation is marked by a gradual change from floodplain-dominated to sandstone facies, a higher degree of channel avulsion, a higher degree of vegetation, a greater degree of channel connectedness, and an increase in channel width. This reflects a climatic change towards greater humidity and precipitation, likely to have altered sediment supply, fluvial processes and basin architecture. The marked differences in facies distribution and architecture between the basal Petaca and Yecua formations on one hand and the megafan-related strata of the Tariquia, Guandacay, and Emborozu formations on the other hand are principally due to tectonic deformation and foreland-ward migration of depositional systems. The preserved Neogene strata show the net cumulative effect of aggradation, transition, and degradation since the Upper Miocene as a response to foreland development, triggered by Andean deformation and uplift.

Acknowledgments

This manuscript is part of a Ph.D. thesis by the first author at the Freie Universität Berlin, Germany. This study was supported by the DFG through its Sonderforschungsbereich (SFB) 267 and by Chaco S.A., Santa Cruz, Bolivia. We thank Oscar Aranibar, Fernando Alegria, and Nigel Robinson of Chaco S.A. for their logistical and material assistance, Luis Buatois (Tucuman, Argentina) for help with trace fossils identification in the field, Achim Schulte (Freie Universität Berlin) for valuable discussions, and Dave Tanner and Sven Egenhoff for proof-reading the manuscript. Thorough reviews by Brian Horton and an anonymous reviewer greatly improved the manuscript.

References

- Allen, J.R.L., 1980. Sand waves: a model of origin and internal structure. *Sedimentary Geology* 26, 281–328.
- Ayaviri, A., 1964. Geología del Área de Tarija, Entre Los Ríos Pilaya–Pilcomayo y Río Bermejo, Informe Interno YPFB (GXG-996).
- Ayaviri, A., 1967. Estratigrafía del Subandino Meridional, Informe Interno YPFB (GXG-1215).
- Baby, P., Hérail, G., Salinas, R., Sempere, T., 1992. Geometry and kinematics evolution of passive roof duplexes deduced from cross-section balancing: example from the foreland thrust system of the southern Bolivian Subandean Zone. *Tectonics* 11, 523–536.
- Baby, P., Specht, M., Oller, J., Montemurro, G., Colletta, B., Letouzey, J., 1994. The Boomerang–Chapare transfer zone (recent oil discovery trend in Bolivia): structural interpretation and experimental approach. *Geodynamic Evolution of Sedimentary Basins*, pp. 203–218.
- Baby, P., Moretti, I., Guillier, B., Limachi, E., Mendez, E., Oller, J., Specht, M., 1995. Petroleum system of the northern and central Bolivian Sub-Andean Zone. In: Tankard, A.J., Suárez Soruco, R., Welsink, H.J. (Eds.), *Petroleum Basins of South America*, Memoir, vol. 62. American Association of Petroleum Geologists, pp. 445–458.
- Baby, P., Rochat, P., Mascle, G., Hérail, G., 1997. Neogene shortening contribution to crustal thickening in the back-arc of the Central Andes. *Geology* 25, 883–886.
- Beck, S.L., Zandt, G., Myers, S.C., Wallace, T.C., Silver, P.G., Drake, L., 1996. Crustal-thickness variations in the central Andes. *Geology* 24, 407–410.
- Belotti, H.J., Saccavino, L.L., Schachner, G.A., 1995. Structural styles and petroleum occurrence in the Subandean fold and thrust belt of northern Argentina. In: Tankard, A.J., Suárez Soruco, R., Welsink, H.J. (Eds.), *Petroleum Basins of South America*, Memoir, vol. 62. American Association of Petroleum Geologists, pp. 545–555.
- Birkett, D.S., 1922. Preliminary Report on Guariri and Saipuru domes, SE Bolivia. Informe interno, vol. 10. Standard Oil Co, Bolivia.
- Blair, T.C., 1999. Sedimentary processes and facies of the waterlaid Anvil Spring Canyon alluvial fan, Death Valley, California. *Sedimentology* 46, 913–940.
- Boothroyd, J.C., Ashley, G.M., 1975. Process, bar morphology and sedimentary structures on braided outwash fans, north-eastern gulf of Alaska. In: Jopling, A.V., McDonald, B.C. (Eds.), *Glaciofluvial and Glaciolacustrine Sedimentation*, vol. 23. Society of Economic Paleontologists and Mineralogists, pp. 193–222.
- Bridge, J.S., 1993. The interaction between channel geometry, water flow, sediment transport and deposition in braided rivers. In: Best, J.L., Bristow, C.S. (Eds.), *Braided Rivers*, Special Publication - Geological Society of London, vol. 75, pp. 13–71.
- Bridge, J.S., 2003. *Rivers and Floodplains: Forms, Processes, and Sedimentary Records*. Blackwell, Oxford. 491 pp.
- Brierley, G.J., Liu, K., Crook, K.A.W., 1993. Sedimentology of coarse-grained alluvial fans in the Markham Valley, Papua New Guinea. *Sedimentary Geology* 86, 297–324.
- Bristow, C.S., 1995. Internal geometry of ancient tidal bedforms revealed using ground penetrating radar. In: Flemming, P.B., Bartholomä, A. (Eds.), *Tidal signatures in modern and ancient sediments*. Special Publication International Association of Sedimentologists, vol. 24, pp. 313–328.
- Buatois, L.A., Uba, C.E., Mángano, G.M., Hulka, C., Heubeck, C., 2004. Deep bioturbation in continental environments: evidence from Miocene fluvial deposits of Bolivia. 1st International Congress on Ichnology, Trelew, Argentina, p. 21.
- Catuneanu, O., Elango, H.N., 2001. Tectonic control on fluvial styles: the Balfour Formation of the Karoo Basin, South Africa. *Sedimentary Geology* 140, 291–313.
- Cecil, C.B., 1990. Paleoclimate controls on stratigraphic repetition of chemical and siliciclastic rocks. *Geology* 18, 533–536.
- Clemente, P., Perez-Arlucea, M., 1993. Depositional architecture of the Cuerda del Pozo Formation, Lower Cretaceous of the extensional Cameros basin, north-central Spain. *Journal of Sedimentology Petrology* 63, 437–452.
- Colletta, B., Letouzey, J., Soares, J., Specht, M., 1999. Detachment versus fault propagation folding: insights from the Subandean Ranges of southern Bolivia. *Thrust Tectonics Congress*, London, pp. 106–109.
- Coudert, L., Frappa, M., Viguier, C., Arias, R., 1995. Tectonic subsidence and crustal flexure in the Neogene Chaco Basin of Bolivia. *Tectonophysics* 243, 277–292.
- Crews, S.G., Ethridge, R.G., 1993. Laramide tectonics and humid alluvial fan sedimentation, NE Unita Uplift, Utah and Wyoming. *Journal of Sedimentology Petrology* 63, 420–436.
- DeCelles, P.G., Cavazza, W., 1999. A comparison of fluvial megafans in the Cordilleran (Upper Cretaceous) and modern Himalayan foreland systems. *Geological Society of America Bulletin* 111, 1315–1334.
- Dunn, J.F., Hartshorn, K.G., Hartshorn, P.W., 1995. Structural styles and hydrocarbon potential of the Subandean thrust belt of southern Bolivia. In: Tankard, A.J., Suárez Soruco, R., Welsink, H.J. (Eds.), *Petroleum Basins of South America*, Memoir, vol. 62. American Association of Petroleum Geologists, pp. 523–543.
- Echavarría, L., Hernández, R., Allmendinger, R., Reynolds, J., 2003. Subandean thrust and fold belt of northwestern Argentina: geometry and timing of the Andean evolution. *American Association of Petroleum Geologists Bulletin* 87, 965–985.
- Ege, H., 2004. Exhumations-und Hebungsgeschichte der zentralen Anden in Südbolivien (21°S) durch Spaltspur-Thermochronologie an Apatit. Ph.D., Thesis, Freie Universität Berlin, Berlin. 159 pp.
- Einsele, G., 2000. *Sedimentary Basins: Evolution, Facies, and Sediment Budget*. Springer, Berlin-Heidelberg. 792 pp.
- Estaban, M., Klappa, C.F., 1983. Subaerial Exposure Environment, Memoir, vol. 33. American Association of Petroleum Geologists, pp. 1–54.
- Ferrell, K.M., 2001. Geomorphology, facies architecture, and high resolution, non-marine sequence stratigraphy in avulsion deposits, Cumberland Marshes, Saskatchewan. *Sedimentary Geology* 139, 93–150.

- Ghosh, S.K., 1987. Cyclicity and facies characteristics of alluvial sediments in the Monongahela-Dunkard Groups, central West Virginia. In: Ethridge, F.G., Flores, R.M., Harvey, M.D. (Eds.), *Recent Developments in Fluvial Sedimentology*, Special Publication Society for Economic, Paleontology and Mineralogy, vol. 31, pp. 229–241.
- Gile, L.H., Peterson, F.F., Grossman, R.B., 1966. Morphological and genetic sequences of carbonate accumulation in desert soils. *Soil Science* 100, 347–360.
- Gubbels, T.L., Isacks, B.L., Farrar, E., 1993. High-level surface, plateau uplift, and foreland development, Bolivian central Andes. *Geology* 21, 695–698.
- Gupta, S., 1999. Controls on sedimentation in distal margin palaeovalleys in the Early Tertiary Alpine foreland basin, south-eastern France. *Sedimentary Geology* 46, 357–384.
- Hérail, G., Oller, J., Baby, P., Bonhomme, M.G., Soler, P., 1996. Strike-slip faulting, thrusting and related basins in Cenozoic evolution of the southern branch of the Bolivian orocline. *Tectonophysics* 259, 201–212.
- Hernandez, R., Reynolds, J., Disalvo, A., 1996. Análisis tectosedimentario y ubicación geocronológica del Grupo Orán en el Río Iruya. *Boletín de Informaciones Petroleras*, Buenos Aires 45, 80–93.
- Horton, B.K., DeCelles, P.G., 2001. Modern and ancient fluvial megafans in the foreland basin system of the central Andes, southern Bolivia: implications for drainage network evolution in fold-thrust belts. *Basin Research* 13, 43–63.
- Hulka, C., Gräfe, K.U., Sames, B., Heubeck, C., Uba, C.E., in press. Depositional setting of the Middle to Upper Miocene Yecua Formation of the central Chaco foreland basin, Bolivia. *Journal of South American Earth Sciences*.
- Husson, L., Moretti, I., 2002. Thermal regime of fold and thrust belts — an application to the Bolivian sub Andean zone. *Tectonophysics* 345, 253–280.
- Isacks, B.L., 1988. Uplift of the central Andean plateau and bending of the Bolivian orocline. *Journal of Geophysical Research* 93, 3211–3231.
- Jimenez-Miranda, F., Lopez-Murillo, R., 1971. *Estratigrafía de Algunas Secciones del Subandino Sur y Centro*, Informe Interno YPF, (GXG-1846).
- Jo, H.R., Rhee, C.W., Chough, S.K., 1997. Distinctive characteristics of a streamflow-dominated alluvial fan deposit: Sanghori area, Kyongsang Basin (Early Cretaceous), southeastern Korea. *Sedimentary Geology* 110, 51–79.
- Jordan, T.E., Reynolds, J.H., Erikson, J.P., 1997. Variability in age of initial shortening and uplift in the central Andes, 16–33°S. In: Ruddima, W.F. (Ed.), *Tectonic Uplift and Climate Change*. Plenum Press, New York, pp. 41–61.
- Khadkikar, A.S., Chamyal, L.S., Ramesh, R., 2000. The character and genesis of calcrete in Upper Quaternary alluvial deposits, Gujarat, western India, and its bearing on the interpretation of ancient climates. *Palaeogeography, Palaeoclimatology, Palaeoecology* 162, 239–261.
- Kirschbaum, M.A., McCabe, P.J., 1992. Controls on the accumulation of coal and on the development of anastomosed fluvial systems in the Cretaceous Dakota Formation of southern Utah. *Sedimentology* 39, 581–598.
- Kleinert, K., Strecker, M.R., 2001. Climate change in response to orographic barrier uplift: paleosol and stable isotope evidence from the late Neogene Santa Maria basin, north-western Argentina. *Geological Society of America Bulletin* 113, 728–742.
- Kley, J., 1996. Transition from basement-involved to thin-skinned thrusting in the Cordillera Oriental of southern Bolivia. *Tectonics* 15, 763–775.
- Kley, J., 1999. Geologic and geometric constraints on a kinematic model of the Bolivian orocline. *Journal of South American Earth Sciences* 12, 221–235.
- Kley, J., Gangui, A.H., Krüger, D., 1996. Basement-involved blind thrusting in the eastern Cordillera Oriental, southern Bolivia: evidence from cross-sectional balancing, gravimetric and magnetotelluric data. *Tectonophysics* 259, 171–184.
- Kley, J., Müller, J., Tawackoli, S., Jacobshagen, V., Manutsoglu, E., 1997. Pre-Andean and Andean-Age deformation in the Eastern Cordillera of Southern Bolivia. *Journal of South American Earth Sciences* 10, 1–19.
- Kley, J., Monaldi, C.R., Salfity, J.A., 1999. Along-strike segmentation of the Andean foreland: causes and consequences. *Tectonophysics* 301, 75–94.
- Kraus, M.J., 2002. Basin-scale changes in floodplain paleosols: implications for interpreting alluvial architecture. *Journal of Sedimentary Research* 72, 500–509.
- Kumar, R., Ghosh, S.K., Mazari, R.K., Sangode, S.J., 2003. Tectonic impact on the fluvial deposits of Plio-Pleistocene Himalayan foreland basin, India. *Sedimentary Geology* 158, 209–234.
- Machette, M.N., 1985. Calcic soils of the south-western United States. *Special Paper - Geological Society of America* 203, 1–21.
- Mack, G.H., James, W.C., Monger, H.C., 1993. Classification of paleosols. *Geological Society of America Bulletin* 105, 129–136.
- Mack, G.H., Leeder, M.R., Perez-Arluca, M., Bailey, B.D.J., 2003. Early Permian silt-bed fluvial sedimentation in the Orogrande basin of the Ancestral Rocky Mountains, New Mexico, USA. *Sedimentary Geology* 160, 159–178.
- Maizels, J., 1989. Sedimentology, paleoflow dynamics and flood history of Jökulhlaup deposits: paleohydrology of Holocene sediment sequences in southern Iceland sandur deposits. *Journal of Geology Petrology* 59, 204–223.
- Makaske, B., Smith, D.G., Berendsen, H.J.A., 2002. Avulsions, channel evolution and floodplain sedimentation rates of the anastomosing upper Columbia River, British Columbia, Canada. *Sedimentology* 49, 1049–1071.
- Marshall, L.G., Sempere, T., 1991. The Eocene to Pleistocene vertebrates of Bolivia and their stratigraphic context: a review. In: Suarez-Soruco, R. (Ed.), *Fosiles y Facies de Bolivia: Vertebrados*, *Revista Técnica de Yacimientos Petrolíferos Fiscales Bolivianos*, vol. 12, pp. 631–652.
- Marshall, L.G., Sempere, T., Gayet, M., 1993. The Petaca (Upper Oligocene–Middle Miocene) and Yecua (Upper Miocene) formations of the Subandean–Chaco basin, Bolivia, and their tectonic significance. *Documents des Laboratoires de Géologie*, Lyon 125, 291–301.

- McCabe, P.J. (Ed.), 1984. Depositional Environments of Coal and Coal-Bearing Strata. *Sedimentology of Coal and Coal-bearing Sequences*, International Association of Sedimentologists, vol. 7, pp. 13–42.
- McCarthy, P.J., Martini, I.P., Leckie, D.A., 1997. Anatomy and evolution of a Lower Cretaceous alluvial plain: sedimentology and paleosols in the upper Blairmore Group, south-western Alberta, Canada. *Sedimentology* 44, 197–220.
- Meisch, C., 2000. Freshwater Ostracoda of Western and Central Europe. Spektrum akademischer Verlag, Heidelberg-Berlin.
- Miall, A.D., 1985. Architectural-element analysis: a new method of facies analysis applied to fluvial deposits. *Earth Science Review* 22, 261–308.
- Miall, A.D., 1996. *The Geology of Fluvial Deposits*. Springer-Verlag, Berlin. 581 pp.
- Moretti, I., Baby, P., Mendez, E., Zubieta, D., 1996. Hydrocarbon generation in relation to thrusting in the Subandean zone from 18° to 22°S, South Bolivia. *Petroleum Geoscience* 2, 17–28.
- Nemec, W., Postma, G., 1993. Quaternary alluvial fans in south-western Crete: sedimentation processes and geomorphic evolution. In: Marzo, M., Puigdefábregas, C. (Eds.), *Alluvial Sedimentation*. International Association of Sedimentologists Special Publication, vol. 17, pp. 235–276.
- Nemec, W., Steel, R.J., 1984. Alluvial and coastal conglomerate: their significant features and some comments on gravelly mass-flow deposits. In: Koster, E.H., Steel, R.J. (Eds.), *Sedimentology of Gravels and Conglomerate*, Memoir, vol. 10. Canadian Society of Petroleum Geologists, pp. 1–31.
- Oller, J., 1986. Consideraciones Generales Sobre la Geología y Estratigrafía de la Faja Subandina Norte., Universite Mayor de San Andres, La Paz. 120 pp.
- Padula, L.E., Reyes, F.C., 1958. Contribución al Léxico Estratigráfico de las Sierras Subandinas, República de Bolivia. *Boletín Técnico de YPF* 1, 9–70.
- Pimentel, N.L., Wright, V.P., Azevedo, T.M., 1996. Distinguishing early groundwater alteration effects from pedogenesis in ancient alluvial basins: examples from the Palaeogene of southern Portugal. *Sedimentary Geology* 105, 1–10.
- Retallack, G.J., 1990. *Soils of the Past: An Introduction to Palaeopedology*. Unwin Hyman, London. 520 pp.
- Retallack, G.J., 1997. *A Color Guide to Paleosols*. Wiley, Chichester. 175 pp.
- Ridgway, K.D., DeCelles, P.G., 1993. Stream-dominated alluvial fan and lacustrine depositional systems in Cenozoic strike-slip basins, Denali fault system, Yukon Territory, Canada. *Sedimentology* 40, 645–666.
- Roeder, D., Chamberlain, R.L., 1995. Structural geology of Sub Andean fold and thrust belt in northwestern Bolivia. In: Tankard, A.J., Suarez, S., Welsink, H.J. (Eds.), *Petroleum Basins of South America*, Memoir, vol. 62. American Association of Petroleum Geologists, pp. 459–479.
- Russo, A., 1959. Estructura y estratigrafía del área de Agua Salada. *Boletín Técnico de YPF* 3, 13–35.
- Rust, B.R., 1981. Sedimentation in an arid-zone anastomosing fluvial system: Cooper's Creek, Central Australia. *Journal of Sedimentary Petrology* 51, 745–755.
- Sempere, T., Hérail, G., Oller, J., Bonhomme, M.G., 1990. Upper Oligocene–Early Miocene major tectonic crisis and related basins in Bolivia. *Geology* 18, 946–949.
- Sheffels, B., 1988. Structural Constraints on Crustal Shortening in the Bolivian Andes. Massachusetts Institute of Technology. 170 pp.
- Sinha, R., Friend, P.F., 1994. River systems and their sediment flux, Indo-Gangetic plains, northern Bihar, India. *Sedimentology* 41, 825–845.
- Smith, D.G., 1983. Anastomosed fluvial deposits: modern examples from western Canada. *Sedimentology* 6, 155–168.
- Smith, D.G., 1986. Anastomosing river deposits, sedimentation rates and basin subsidence, Magdalena River, northwestern Columbia, South America. *Sedimentary Geology* 46, 177–196.
- Smith, D.G., Smith, N.D., 1980. Sedimentation in anastomosed river systems: examples from alluvial valleys near Banff, Alberta. *Journal of Sedimentary Petrology* 50, 157–164.
- Smith, N.D., Cross, T.A., Dufficy, J.P., Clough, S.R., 1989. Anatomy of an avulsion. *Sedimentology* 36, 1–24.
- Smoot, J.P., 1983. Depositional subenvironments in an arid closed basin; the Wilkins Peak Member of the Green River Formation (Eocene), Wyoming, USA. *Sedimentology* 30, 801–827.
- Starck, D., Anzótégui, L.M., 2001. The Late Miocene climate change-persistence of climatic signal through the orogenic stratigraphic record in northwestern Argentina. *Journal of South American Earth Sciences* 14, 763–774.
- Stear, W.M., 1985. Comparison of the bedform distribution and dynamics of modern and ancient sandy ephemeral flood deposits in the southwestern Karoo region, South Africa. *Sedimentary Geology* 45, 209–230.
- Steel, R.J., Maehle, S., Nilsen, H., Roe, S.L., Spinnanger, A., 1977. Coarsening-upward cycles in the alluvium of Hornelen Basin (Devonian) Norway: sedimentary response to tectonic events. *Geological Society of America Bulletin* 88, 1124–1134.
- Suarez Soruco, R., 1999. Léxico Estratigráfico de Bolivia. *Revista Técnica de YPF*.
- Todd, S.P., 1989. Stream-driven, high-density gravelly traction carpets: possible deposits in the Trabeg Conglomerate Formation, SW Ireland and theoretical considerations of their origin. *Sedimentology* 36, 513–530.
- Todd, S.P., 1996. Process deduction from fluvial sedimentary structures. In: Carling, P.A., Dawson, M.R. (Eds.), *Advances in Fluvial Dynamics and Stratigraphy*. Wiley, Chichester, pp. 299–350.
- Tooth, S., Nanson, G.C., 2004. Forms and processes of two highly contrasting rivers in arid central Australia, and the implication for channel-pattern discrimination and prediction. *Geological Society of America Bulletin* 116, 802–816.
- Turner, P., 1980. *Continental Red Beds*. Elsevier, Amsterdam. 562 pp.
- Uba, C.E., Heubeck, C., 2003. Evolution of the southern part of the Tertiary Chaco foreland basin, southern Bolivia. 3rd Latinamerican Sedimentological Congress, Belem, Brazil, p. 189.
- Uba, C.E., Heubeck, C., Hulka, C., submitted for publication. Thrust belt-foreland basin interaction from integrated outcrop and seismic data in the Late Cenozoic Chaco basin, Bolivia. *Basin Research*.

- Wells, N.A., Dorr, J.A.J., 1987. Shifting of the Kosi River, northern India. *Geology* 15, 204–207.
- Welsink, H.J., Martinez, E., Aranibar, O., Jarandilla, J., 1995. Structural inversion of a Cretaceous rift basin, southern Altiplano, Bolivia. In: Tankard, A.J., Suárez-Soruco, R., Welsink, H.J. (Eds.), *Petroleum Basins of South America*, Memoir, vol. 62. American Association of Petroleum Geologists, pp. 305–324.
- Wright, V.P., 1994. Paleosols in shallow marine carbonate sequences. *Earth Science Review* 35, 367–395.
- Wright, V.P., Tucker, M.E., 1991. Calcrete. Reprint Series of the International Association of Sedimentologists, vol. 2. 352 pp.